

Policy-Aware Model Learning for Policy Gradient Methods

Romina Abachi* Mohammad Ghavamzadeh[†] Amir-massoud Farahmand[‡]

Abstract

This paper considers the problem of learning a model in model-based reinforcement learning (MBRL). We examine how the planning module of an MBRL algorithm uses the model, and propose that the model learning module should incorporate the way the planner is going to use the model. This is in contrast to conventional model learning approaches, such as those based on maximum likelihood estimate, that learn a predictive model of the environment without explicitly considering the interaction of the model and the planner. We focus on policy gradient type of planning algorithms and derive new loss functions for model learning that incorporate how the planner uses the model. We call this approach Policy-Aware Model Learning (PAML). We theoretically analyze a generic model-based policy gradient algorithm and provide a convergence guarantee for the optimized policy. We also empirically evaluate PAML on some benchmark problems, showing promising results.

1 Introduction

A model-based reinforcement learning (MBRL) agent gradually learns a model of the environment as it interacts with it, and uses the learned model to plan and find a good policy. This can be done by planning with samples coming from the model, instead of or in addition to the samples from the environment, e.g., Sutton (1990); Peng & Williams (1993); Sutton et al. (2008); Deisenroth et al. (2015); Talvitie (2017); Ha & Schmidhuber (2018). If learning a model is easier than learning the policy or value function in a model-free manner, MBRL will lead to a reduction in the number of required interactions with the real-world and will improve the sample complexity of the agent. However, this is contingent on the ability of the agent to learn an accurate model of the real environment. Therefore, the problem of learning a good model of the environment is of paramount importance in the success of MBRL. This paper addresses the question of how we can approach the problem of learning a model of the environment, and proposes a method called *policy-aware model learning* (PAML).

The conventional approach to model learning in MBRL is to learn a model that is a good predictor of the environment. If the learned model is accurate enough, this leads to a value function or a policy that is close to the optimal one. Learning a good predictive model can be achieved by minimizing some form of a probabilistic loss. A common choice is to minimize the KL-divergence

*Department of Electrical and Computer Engineering, University of Toronto & the Vector Institute, Toronto, Canada

[†]Facebook AI Research, CA, USA

[‡]The Vector Institute & the Department of Computer Science and the Department of Mechanical and Industrial Engineering, University of Toronto, Toronto, Canada

between the empirical data and the model, which leads to the Maximum Likelihood Estimator (MLE).

The often-unnoticed fact, however, is that no model can be completely accurate, and there are always differences between the model and the real-world. An important source of inaccuracy/error is the choice of model space, i.e., the space of predictors, such as a particular class of deep neural networks. We suffer an error if the model space does not contain the true model of the physical system.

The *decision-aware model learning* (DAML) viewpoint suggests that instead of trying to learn a model that is a good predictor of the environment, which may not be possible as just argued, one should learn only those aspects of the environment that are relevant to the decision problem. Trying to learn the complex dynamics that are irrelevant to the underlying decision problem is pointless, e.g., in a self-driving car, the agent does not need to model the movement of the leaves on trees when the decision problem is simply to decide whether or not to stop at a red light. The conventional model learning approach cannot distinguish between decision-relevant and irrelevant aspects of the environment, and may waste the “capacity” of the model on unnecessary details. In order to focus the model on the decision-relevant aspects, we shall incorporate certain aspects of the decision problem into the model learning process.

Value-Aware Model Learning (VAML) is an instantiation of DAML that incorporates the information about the value function in learning the model of the environment (Farahmand et al., 2017; Farahmand, 2018). The formulation by Farahmand et al. (2017) incorporates the knowledge about the *value function space* in learning the model, and the formulation by Farahmand (2018) benefits from how the value functions are generated within an approximate value iteration (AVI)-based MBRL agent. We explain the VAML framework in more details in Section 2. There are a few other relatively recent works that can be interpreted as doing DAML, even though they do not always explicitly express their goal as such. Some examples are Joseph et al. (2013); Silver et al. (2017b); Oh et al. (2017); Farquhar et al. (2018); Luo et al. (2018); D’Oro et al. (2019).

Designing a decision-aware model learning approach, however, is not limited to methods that benefit from the structure of the value function. Policy is another main component of RL that can be exploited for learning a model. The high-level idea is simple: If we are using a policy gradient (PG) method to search for a good policy, we only need to learn a model that provides accurate estimates of the PG. All other details of the environment that do not contribute to estimating PG are irrelevant. Formalizing this intuition is the main algorithmic contribution of this paper (Section 3).

The first theoretical contribution of this work is a result that shows how the error in the model, in terms of total variation, affects the quality of the PG estimate (Theorem 2 in Section 4.1). This is reassuring as it shows that a good model leads to an accurate estimate of the PG. It might seem natural to assume that an accurate gradient estimate leads to convergence to a good policy. However, we could not quantify the quality of the converged policy in a PG procedure beyond stating that it is a local optimum until recently, when Agarwal et al. (2019) provided quantitative guarantees on the convergence of PG methods beyond convergence to a local optimum. Our second theoretical contribution is Theorem 5 (Section 4.2) that extends one of the results in Agarwal et al. (2019) to model-based PG and shows the effect of model error on the quality of the converged policy, as compared to the best policy in the policy class. We also have a subtle, but perhaps important, technical contribution in the definition of the policy approximation error, which holds even in the original model-free setting.

Our empirical contributions are demonstrating that PAML can easily be formulated for two

Algorithm 1 Generic MBRL Algorithm

Initialize a policy π_0
for $k = 0, 1, \dots, K$ **do**
 Generate training set $\mathcal{D}_n^{(k)} = \{(X_i, A_i, R_i, X'_i)\}_{i=1}^n$ by interacting with the true environment (potentially using π_k), i.e., $(X_i, A_i) \sim \nu_k$ with $X'_i \sim \mathcal{P}^*(\cdot|X_i, A_i)$ and $R_i \sim \mathcal{R}^*(\cdot|X_i, A_i)$.
 $\hat{\mathcal{P}}^{(k+1)} \leftarrow \operatorname{argmin}_{\mathcal{P} \in \mathcal{M}} \operatorname{Loss}_{\mathcal{P}}(\mathcal{P}; \cup_{i=0}^k \mathcal{D}_n^{(i)})$ {PAML: $\operatorname{Loss}_{\mathcal{P}} = \|\nabla_{\theta} J(\mu_{\theta}^k) - \nabla_{\theta} \hat{J}(\mu_{\theta}^k)\|_{\cup_{i=0}^k \mathcal{D}_n^{(i)}}^2$ }
 $\hat{r} \leftarrow \operatorname{argmin}_{r \in \mathcal{G}} \operatorname{Loss}_{\mathcal{R}}(r; \cup_{i=0}^k \mathcal{D}_n^{(i)})$
 $\pi_{\theta}^{k+1} \leftarrow \operatorname{Planner}(\hat{\mathcal{P}}, \hat{\mathcal{R}})$ {PAML: PG-based (e.g., REINFORCE or DDPG); $\theta_{k+1} \leftarrow \theta_k + \eta \nabla_{\theta} \hat{J}(\pi_{\theta}^k)$.}
end for, {Return π_K }

commonly-used PG algorithms and showing its performance in benchmark environments (Section 5), for which the code is made available at <https://github.com/romina72/paml>. In addition, our results in a finite-state environment show that PAML outperforms conventional methods when the model capacity is limited.

2 Background on Value-Aware Model Learning (VAML)

A MBRL agent interacts with an environment, collects data, improves its internal model, and uses the internal model, perhaps alongside the real-data, to improve its policy. To formalize, we consider a (discounted) Markov Decision Process (MDP) $(\mathcal{X}, \mathcal{A}, \mathcal{R}^*, \mathcal{P}^*, \gamma)$ (Szepesvári, 2010). We denote the state space by \mathcal{X} , the action space by \mathcal{A} , the reward distribution by \mathcal{R}^* , the transition probability kernel by \mathcal{P}^* , and the discount factor by $0 \leq \gamma \leq 1$. In general, the true transition model \mathcal{P}^* and the reward distribution \mathcal{R}^* are not known to an RL agent. The agent instead can interact with the environment to collect samples from these distributions. The collected data is in the form of

$$\mathcal{D}_n = \{(X_i, A_i, R_i, X'_i)\}_{i=1}^n, \quad (1)$$

with the current state-action being distributed according to $Z_i = (X_i, A_i) \sim \nu(\mathcal{X} \times \mathcal{A}) \in \bar{\mathcal{M}}(\mathcal{X} \times \mathcal{A})$, the reward $R_i \sim \mathcal{R}^*(\cdot|X_i, A_i)$, and the next-state $X'_i \sim \mathcal{P}^*(\cdot|X_i, A_i)$. Note that $\bar{\mathcal{M}}$ refers to the set of all probability distributions defined over \mathcal{X} and \mathcal{A} . In many cases, an RL agent might follow a trajectory X_1, X_2, \dots in the state space (and similar for actions and rewards), that is, $X_{i+1} = X'_i$. We denote the expected reward by $r^*(x, a) = \mathbb{E}[\mathcal{R}^*(\cdot|x, a)]$.¹

A MBRL agent uses the interaction data to learn an estimate $\hat{\mathcal{P}}$ of the true model \mathcal{P}^* and $\hat{\mathcal{R}}$ (or simply \hat{r}) of the true reward distribution \mathcal{R}^* (or r^*). This is called *model learning*. These models are then used by a planning algorithm `Planner` to find a close-to-optimal policy. The policy may be used by the agent to collect more data and improve the estimates $\hat{\mathcal{P}}$ and $\hat{\mathcal{R}}$. This generic Dyna-style (Sutton, 1990) MBRL algorithm is shown in Algorithm 1.

How should we learn a model $\hat{\mathcal{P}}$ that is most suitable for a particular `Planner`? This is the fundamental question in model learning. The conventional approach in model learning ignores how `Planner` is going to use the model and instead focuses on learning a good predictor of the environment. This can be realized by using a probabilistic loss, such as KL-divergence, which leads to the maximum likelihood estimate (MLE), or similar approaches. Ignoring how the planner uses the model, however, might not be a good idea, especially if the model class \mathcal{M} , from which we select

¹Given a set Ω and its σ -algebra σ_{Ω} , $\bar{\mathcal{M}}(\Omega)$ refers to the set of all probability distributions defined over σ_{Ω} . As we do not get involved in the measure theoretic issues in this paper, we do not explicitly define the σ -algebra, and simply use a well-defined and “standard” one, e.g., Borel sets defined for metric spaces.

our estimate $\hat{\mathcal{P}}$, does not contain the true model \mathcal{P}^* , i.e., $\mathcal{P}^* \notin \mathcal{M}$. This is the model approximation error and its consequence is that we cannot capture all aspects of the dynamics. The thesis behind DAML is that instead of being oblivious to how Planner uses the model, the model learner should pay more attention to those aspects of the model that affect the decision problem the most. A purely probabilistic loss ignores the underlying decision problem and how Planner uses the learned model, whereas a DAML method incorporates the decision problem and Planner.

Value-Aware Model Learning (VAML) is a class of DAML methods (Farahmand et al., 2016a, 2017; Farahmand, 2018). It is a model learning approach that is designed for a value-based type of Planner, i.e., a planner that finds a good policy by approximating the optimal value function Q^* by \hat{Q}^* , and then computes the greedy policy w.r.t. \hat{Q}^* . In particular, the suggested formulations of VAML so far focus on value-based methods that use the Bellman optimality operator to find the optimal value function (as opposed to a Monte Carlo-based solution). The use of the Bellman [optimality] operator, or a sample-based approximation thereof, is a key component of many value-based approaches, such as the family of (Approximate) Value Iteration (Gordon, 1995; Szepesvári & Smart, 2004; Ernst et al., 2005; Munos & Szepesvári, 2008; Farahmand et al., 2009; Farahmand & Precup, 2012; Mnih et al., 2015; Tosatto et al., 2017; Chen & Jiang, 2019) or (Approximate) Policy Iteration (API) algorithms (Lagoudakis & Parr, 2003a; Antos et al., 2008; Bertsekas, 2011; Lazaric et al., 2012; Scherrer et al., 2012; Farahmand et al., 2016b).

To be more concrete in the description of VAML, let us first recall that the Bellman optimality operator w.r.t. the transition kernel \mathcal{P} is defined as

$$T_{\mathcal{P}}^* : Q \mapsto r + \gamma \mathcal{P} \max_a Q. \quad (2)$$

VAML attempts to find $\hat{\mathcal{P}}$ such that applying the Bellman operator $T_{\hat{\mathcal{P}}}^*$ according to the model $\hat{\mathcal{P}}$ on a value function Q has a similar effect as applying the true Bellman operator $T_{\mathcal{P}^*}^*$ on the same function, i.e., $T_{\hat{\mathcal{P}}}^* Q \approx T_{\mathcal{P}^*}^* Q$. This ensures that one can replace the true dynamics with the model without (much) affecting the internal mechanism of a Bellman operator-based Planner. How this might be achieved is described in the original papers, which are summarized in Appendix B.

The VAML framework is an instantiation of DAML when Planner benefits from extra knowledge available about the value function, either in the form of the value function space (as in the original VAML formulation) or particular value functions generated by AVI (as in the IterVAML formulation), to learn a model $\hat{\mathcal{P}}$. The value function and our knowledge about it, however, are not the only extra information that we might have about the decision problem. Another source of information is the policy. The goal of the next section is to develop a model learning framework that benefits from the properties of the policy.

3 Policy-Aware Model Learning

The policy gradient (PG) algorithm and its several variants are important tools to solve RL problems (Williams, 1992; Sutton et al., 2000; Baxter & Bartlett, 2001; Marbach & Tsitsiklis, 2001; Kakade, 2001; Peters et al., 2003; Cao, 2005; Ghavamzadeh & Engel, 2007; Peters & Schaal, 2008; Bhatnagar et al., 2009; Deisenroth et al., 2013; Schulman et al., 2015). These algorithms parameterize the policy and compute the gradient of the performance (cf. (4)) w.r.t. the parameters. Model-free PG algorithms use the environment to estimate the gradient, but model-based ones use an estimated $\hat{\mathcal{P}}$ to generate “virtual” samples to estimate the gradient. Refer to Deisenroth et al. (2013) and references therein for more information about PG algorithms. In this section, we derive

a loss function for model learning that is designed for model-based PG estimation. We specialize the derivation to discounted MDPs, but the changes for the episodic, finite-horizon, or average reward MDPs should be straightforward.

A PG method relies on accurate estimation of the gradient. Intuitively, a model-based PG method would perform well if the gradient of the performance evaluated according to the model $\hat{\mathcal{P}}$ is close to the one computed from the true dynamics \mathcal{P}^* . In this case, one may use the learned model instead of the true environment to compute the PG. To formalize this intuition, we first introduce some notations.

Given a transition probability kernel \mathcal{P}^π , we denote by $\mathcal{P}^\pi(\cdot|x;k)$, the future-state distribution of following policy π from state x for k steps, i.e., $\mathcal{P}^\pi(\cdot|x;k) \triangleq (\mathcal{P}^\pi)^k(\cdot|x)$, with the understanding that $(\mathcal{P}^\pi)^0(\cdot|x) = \mathbf{I}$ is the identity map. For an initial probability distribution $\rho \in \mathcal{M}(\mathcal{X})$, $\int \rho(dx)\mathcal{P}^\pi(\cdot|x;k)$ is the distribution of selecting the initial distribution according to ρ and following \mathcal{P}^π for k steps. We define a discounted future-state distribution of starting from ρ and following \mathcal{P}^π as

$$\rho_\gamma^\pi(\cdot) = \rho_\gamma(\cdot; \mathcal{P}^\pi) \triangleq (1 - \gamma) \sum_{k \geq 0} \gamma^k \int d\rho(x)\mathcal{P}^\pi(\cdot|x;k). \quad (3)$$

We may drop the dependence on π , if it is clear from the context. We use a shorthand notation $\hat{\rho}_\gamma^\pi = \rho_\gamma(\cdot; \hat{\mathcal{P}}^\pi)$, and a similar notation for other distributions, e.g., μ_γ^π and $\hat{\mu}_\gamma^\pi$.

For an MDP $(\mathcal{X}, \mathcal{A}, \mathcal{R}^*, \mathcal{P}, \gamma)$, we use the subscript \mathcal{P} in the definition of value function $V_{\mathcal{P}}^\pi$ and $Q_{\mathcal{P}}^\pi$, if we want to emphasize its dependence on the transition probability kernel. We reserve the use of V^π and Q^π for $V_{\mathcal{P}^*}^\pi$ and $Q_{\mathcal{P}^*}^\pi$, the value functions of the true dynamics.

The performance of an agent starting from a user-defined initial probability distribution $\rho \in \mathcal{M}(\mathcal{X})$, following policy π in the true MDP $(\mathcal{X}, \mathcal{A}, \mathcal{R}^*, \mathcal{P}^*, \gamma)$ is

$$J(\pi) = J_\rho(\pi) = \int d\rho(x)V^\pi(x). \quad (4)$$

When the policy $\pi = \pi_\theta$ is parameterized by $\theta \in \Theta$, from the derivation of the PG theorem (cf. proof of Theorem 1 by [Sutton et al. 2000](#)), we have that

$$\frac{\partial V^{\pi_\theta}(x)}{\partial \theta} = \sum_{k \geq 0} \gamma^k \int \mathcal{P}^{*\pi_\theta}(dx'|x;k) \sum_{a' \in \mathcal{A}} \frac{\partial \pi_\theta(a'|x')}{\partial \theta} Q_{\mathcal{P}^*}^{\pi_\theta}(x', a'),$$

If the dependence of Q on the transition kernel is clear, we may omit it and simply use Q^{π_θ} . We also use \mathcal{P}^{π_θ} instead of $\mathcal{P}^{*\pi_\theta}$ to simplify the notation. The gradient of the performance $J(\pi_\theta)$ (4) w.r.t. θ is then

$$\begin{aligned} \nabla_\theta J(\pi_\theta) &= \frac{\partial J(\pi_\theta)}{\partial \theta} = \sum_{k \geq 0} \gamma^k \int d\rho(x) \int \mathcal{P}^{\pi_\theta}(dx'|x;k) \sum_{a' \in \mathcal{A}} \frac{\partial \pi_\theta(a'|x')}{\partial \theta} Q^{\pi_\theta}(x', a') \\ &= \frac{1}{1 - \gamma} \int \rho_\gamma(dx; \mathcal{P}^{\pi_\theta}) \sum_{a \in \mathcal{A}} \pi_\theta(a|x) \frac{\partial \log \pi_\theta(a|x)}{\partial \theta} Q^{\pi_\theta}(x, a). \end{aligned} \quad (5)$$

Let us define an auxiliary function g , which shall help us easily describing several ways a model-based PG method can be devised. For two transition probability kernels \mathcal{P}_1 and \mathcal{P}_2 , and a policy

π_θ , we define

$$g(\pi_\theta; \mathcal{P}_1, \mathcal{P}_2) = \sum_{k \geq 0} \gamma^k \int d\rho(x) \int \mathcal{P}_1^{\pi_\theta}(dx'|x; k) \sum_{a' \in \mathcal{A}} \frac{\partial \pi_\theta(a'|x')}{\partial \theta} Q_{\mathcal{P}_2}^{\pi_\theta}(x', a'). \quad (6)$$

This vector-valued function can be seen as the PG of following π_θ according to \mathcal{P}_1 , and using a critic that is the value function in an MDP with \mathcal{P}_2 as the transition kernel. It is clear that $\nabla_\theta J(\pi_\theta) = g(\pi_\theta; \mathcal{P}^*, \mathcal{P}^*)$.

We have several choices to design a model learning loss function that is suitable for a PG method. The overall goal is to match the true PG, i.e., $\frac{\partial J(\pi)}{\partial \theta} = g(\pi_\theta; \mathcal{P}^*, \mathcal{P}^*)$, or an empirical estimate thereof, with a PG that is somehow computed by the model $\hat{\mathcal{P}}$. Let us define $\frac{\partial \hat{J}(\pi)}{\partial \theta} \triangleq g(\pi_\theta; \hat{\mathcal{P}}, \mathcal{P}^*)$ and set the goal of model learning to

$$\frac{\partial J(\pi_\theta)}{\partial \theta} \approx \frac{\partial \hat{J}(\pi_\theta)}{\partial \theta}. \quad (7)$$

This ensures that the gradient estimate based on following the learned model $\hat{\mathcal{P}}^{\pi_\theta}$ and computed using the true action-value function $Q_{\mathcal{P}^*}^{\pi_\theta}$ is close to the true gradient. There are various ways to quantify the error between the gradient vectors. We choose the ℓ_2 -norm of their difference. When the gradient w.r.t. the model is close to the true gradient, we may use the model to perform PG and the updated policies would be similar.

Subtracting the gradient of the performances under two different transition probability kernels and taking the ℓ_2 -norm, we get a loss function between the true and model PGs, i.e.,

$$\begin{aligned} c_\rho(\mathcal{P}^{\pi_\theta}, \hat{\mathcal{P}}^{\pi_\theta}) &= \left\| \frac{\partial J(\pi_\theta)}{\partial \theta} - \frac{\partial \hat{J}(\pi_\theta)}{\partial \theta} \right\|_2 \\ &= \left\| \sum_{k \geq 0} \gamma^k \int d\rho(x) \int (\mathcal{P}^{\pi_\theta}(dx'|x; k) - \hat{\mathcal{P}}^{\pi_\theta}(dx'|x; k)) \sum_{a' \in \mathcal{A}} \frac{\partial \pi_\theta(a|x')}{\partial \theta} Q^{\pi_\theta}(x', a') \right\|_2. \end{aligned} \quad (8)$$

Note that the summation (or integral) over actions $\sum_{a' \in \mathcal{A}} \frac{\partial \pi_\theta(a|x')}{\partial \theta} Q^{\pi_\theta}(x', a')$ is identical to $\mathbb{E}_{A' \sim \pi_\theta(\cdot|x')} [\nabla_\theta \log \pi_\theta(A'|x) Q^{\pi_\theta}(x', A')]$.

Several comments are in order. This is a population loss function, in the sense that \mathcal{P} appears in it. To make this loss practical, we need to use its empirical version. Moreover, this formulation requires us to know the action-value function $Q^{\pi_\theta} = Q_{\mathcal{P}^*}^{\pi_\theta}$, which is w.r.t. the true dynamics. This can be estimated using a model-free critic that only uses the real transition data (and not the data obtained by the model $\hat{\mathcal{P}}^\pi$) and provides $\hat{Q}^{\pi_\theta} \approx Q_{\mathcal{P}^*}^{\pi_\theta}$. To be concrete, let us assume that we are given n episodes with length T of following policy \mathcal{P}^{π_θ} starting from an initial state distribution ρ . That is, $X_1^{(i)} \sim \rho$, $A_k^{(i)} \sim \pi_\theta(\cdot|X_k^{(i)})$ and $X_{k+1}^{(i)} \sim \mathcal{P}^*(\cdot|X_k^{(i)}, A_k^{(i)})$ for $k = 0, \dots, T-1$ and $i = 1, \dots, n$. In order to compute the expectation w.r.t. $\hat{\rho}_\gamma$, we generate samples from $\hat{\mathcal{P}}^{\pi_\theta}$ as follows: For each $i = 1, \dots, n$ and $j = 1, \dots, m$, we set $\tilde{X}_{1,j}^{(i)} = X_1^{(i)}$ (the same initial states as in the real data). And for the next steps, we let $\tilde{A}_{k,j}^{(i)} \sim \pi_\theta(\cdot|X_k^{(i)})$ and $\tilde{X}_{k+1,j}^{(i)} \sim \hat{\mathcal{P}}(\cdot|\tilde{X}_{k,j}^{(i)}, \tilde{A}_{k,j}^{(i)})$ (which

should be interpreted as the same model as $\hat{\mathcal{P}}^{\pi_\theta}$ for $i = 1, \dots, n$, $j = 1, \dots, m$, and $k = 0, \dots, T-1$. The empirical loss can then be defined as

$$c_n(\mathcal{P}^{\pi_\theta}, \hat{\mathcal{P}}^{\pi_\theta}) = \left\| \frac{1}{n} \sum_{i=1}^n \sum_{k=1}^T \gamma^k \left[\nabla_\theta \log \pi_\theta(A_k^{(i)} | X_k^{(i)}) \hat{Q}^{\pi_\theta}(X_k^{(i)}, A_k^{(i)}) - \frac{1}{m} \sum_{j=1}^m \nabla_\theta \log \pi_\theta(\tilde{A}_{k,j}^{(i)} | X_k^{(i)}) \hat{Q}^{\pi_\theta}(X_{k,j}^{(i)}, \tilde{A}_{k,j}^{(i)}) \right] \right\|_2. \quad (9)$$

Also note the loss function $c_\rho(\mathcal{P}^{\pi_\theta}, \hat{\mathcal{P}}^{\pi_\theta})$ (8) (and its empirical version) is defined for a particular policy π_θ . However, policy π_θ gradually changes during the running of a PG algorithm. To deal with this change, we should regularly update $\hat{\mathcal{P}}^{\pi_\theta}$ based on data collected by the most recent π_θ .

Setting $g(\pi_\theta; \mathcal{P}^*, \mathcal{P}^*) \approx g(\pi_\theta; \hat{\mathcal{P}}, \mathcal{P}^*)$ is only one way to define a model learning objective for a PG method. We can require to find a $\hat{\mathcal{P}}$ such that

$$\frac{\partial J(\pi)}{\partial \theta} = g(\pi_\theta; \mathcal{P}^*, \mathcal{P}^*) \approx \begin{cases} g(\pi_\theta; \hat{\mathcal{P}}, \mathcal{P}^*), & (10a) \\ g(\pi_\theta; \mathcal{P}^*, \hat{\mathcal{P}}), & (10b) \\ g(\pi_\theta; \hat{\mathcal{P}}, \hat{\mathcal{P}}). & (10c) \end{cases}$$

The difference between these cases is in whether the discounted future-state distribution is computed according to the true dynamics \mathcal{P}^* or the learned dynamics $\hat{\mathcal{P}}$, and whether the critic $Q_{\mathcal{P}}^{\pi_\theta}$ is computed according to the true dynamics or the learned dynamics. Case (10a) is the same as (7). Case (10b) uses the model only to train the critic, but does not use the learned model to compute the future-state distribution $\hat{\rho}_\gamma$ in matching the PG obtained by the model and the true dynamics. Having $\hat{\mathcal{P}}$, the critic can be estimated using Monte Carlo estimates or any other method for estimating the value function given a model. This is similar to how [D’Oro et al. \(2019\)](#) use their model, though their loss function is different, in that the model-learning step does not take the action-value function into account. Case (10c) corresponds to the PG according to the model $\hat{\mathcal{P}}^\pi$. This requires us to estimate both the future-state distribution and the critic according to the model. In this paper, we theoretically analyze (10a) and provide empirical results for approximations of (10a) and (10b).

If the policy is deterministic ([Silver et al., 2014](#)), the formulation would be almost the same with the difference that instead of terms in the form of $\sum_{a \in \mathcal{A}} \nabla_\theta \pi_\theta(a|x) Q^{\pi_\theta}(x, a)$, we would have $\nabla_\theta \pi_\theta(x) \frac{\partial Q^{\pi_\theta}(x, a)}{\partial a} |_{a=\pi_\theta(x)}$. In our experiments in Section 5, we show results for the planners that use deep deterministic policy gradient (DDPG) ([Lillicrap et al., 2015](#)) and REINFORCE ([Williams, 1992](#)) algorithms. Other planners, such as TRPO ([Schulman et al., 2015](#)), may also be used with a corresponding PAML loss. We leave studying them for future work.

4 Theoretical Analysis of PAML

We theoretically study some aspects of a generic model-based PG (MBPG) method. Theorem 2 in Section 4.1 quantifies the error between the PG $\nabla_\theta J(\pi_\theta)$ obtained by following the true model \mathcal{P}^* and the PG $\nabla_\theta \hat{J}(\pi_\theta)$ obtained by following $\hat{\mathcal{P}}$, and relates it to the error between the models. Even though having a small PG error might intuitively suggest that using $\nabla_\theta \hat{J}(\pi_\theta)$ instead of $\nabla_\theta J(\pi_\theta)$ should lead to a good policy, it does not show the quality of the converged policy. Theorem 4 in

Section 4.2 provides such a convergence guarantee for a MB PG and shows that having a small PG error indeed leads to a better solution. The results of this section are for a generic MBPG method, but we can draw conclusions about PAML and why it might be a better approach compared to a conventional MLE-based model learning.

4.1 Policy Gradient Error

Given the true $\mathcal{P} = \mathcal{P}^*$ and estimated $\hat{\mathcal{P}}$ transition probability kernel, a policy π_θ , and their induced discounted future-state distributions $\rho_\gamma^{\pi_\theta} = \rho_\gamma(\cdot; \mathcal{P}^{\pi_\theta})$ and $\hat{\rho}_\gamma^{\pi_\theta} = \rho_\gamma(\cdot; \hat{\mathcal{P}}^{\pi_\theta})$, the performance gradients $\frac{\partial J(\pi_\theta)}{\partial \theta}$ (according to \mathcal{P}^{π_θ}) and $\frac{\partial \hat{J}(\pi_\theta)}{\partial \theta}$ (according to $\hat{\mathcal{P}}^{\pi_\theta}$) are

$$\begin{aligned}\frac{\partial J(\pi_\theta)}{\partial \theta} &= \frac{1}{1-\gamma} \mathbb{E}_{X \sim \rho_\gamma(\cdot; \mathcal{P}^{\pi_\theta})} \left[\mathbb{E}_{A \sim \pi_\theta(\cdot|X)} [\nabla_\theta \log \pi_\theta(A|X) Q^{\pi_\theta}(X, A)] \right], \\ \frac{\partial \hat{J}(\pi_\theta)}{\partial \theta} &= \frac{1}{1-\gamma} \mathbb{E}_{X \sim \rho_\gamma(\cdot; \hat{\mathcal{P}}^{\pi_\theta})} \left[\mathbb{E}_{A \sim \pi_\theta(\cdot|X)} [\nabla_\theta \log \pi_\theta(A|X) Q^{\pi_\theta}(X, A)] \right].\end{aligned}\quad (11)$$

We want to compare the difference of these two PG. Recall that this is the case when the same critic $Q^{\pi_\theta} = Q_{\mathcal{P}}^{\pi_\theta}$ is used for both PG calculation, e.g., a critic is learned in a model-free way, and not based on $\hat{\mathcal{P}}$. Also we assume that the critic is exact, and we do not consider that one should learn it based on data, which brings in considerations on the approximation and estimation errors for a policy evaluation method. Theoretical analyses on how well we might learn a critic have been studied before.

We first introduce some notations and definitions. Let us denote $\Delta \mathcal{P}^\pi = \mathcal{P}^\pi - \hat{\mathcal{P}}^\pi$. For the error in transition kernel $\Delta \mathcal{P}^\pi(\cdot|x)$, which is a signed measure, we use $\|\Delta \mathcal{P}^\pi(\cdot|x)\|_1$ to denote its total variation (TV) distance, i.e., $\|\Delta \mathcal{P}^\pi(\cdot|x)\|_1 = 2 \sup_{A \in \mathcal{X}} |\int \Delta \mathcal{P}^\pi(dy|x) \mathbb{I}\{y \in A\}|$, where the supremum is over the measurable subsets of \mathcal{X} . We have

$$\|\Delta \mathcal{P}^\pi(\cdot|x)\|_1 = \sup_{\|f\|_\infty \leq 1} \left| \int \Delta \mathcal{P}^\pi(dy|x) f(y) \right|, \quad (12)$$

where the supremum is over 1-bounded measurable functions on \mathcal{X} . When $\Delta \mathcal{P}^\pi(\cdot|x)$ has a density w.r.t. to some countably additive non-negative measure, it holds that $\|\Delta \mathcal{P}^\pi(\cdot|x)\|_1 = \int |\Delta \mathcal{P}^\pi(dy|x)|$.

We define the following two norms on $\Delta \mathcal{P}^\pi$: Consider a probability distribution $\nu \in \bar{\mathcal{M}}(\mathcal{X})$. We define

$$\|\Delta \mathcal{P}^\pi\|_{1,\infty} = \sup_{x \in \mathcal{X}} \|\Delta \mathcal{P}^\pi(\cdot|x)\|_1, \quad \|\Delta \mathcal{P}^\pi\|_{1,1(\nu)} = \int d\nu(x) \|\Delta \mathcal{P}^\pi(\cdot|x)\|_1.$$

We also define

$$\text{KL}_\infty(\mathcal{P}_1^\pi \| \mathcal{P}_2^\pi) = \sup_{x \in \mathcal{X}} \text{KL}(\mathcal{P}_1^\pi(\cdot|x) \| \mathcal{P}_2^\pi(\cdot|x)), \quad \text{KL}_{1(\nu)}(\mathcal{P}_1^\pi \| \mathcal{P}_2^\pi) = \int d\nu(x) \text{KL}(\mathcal{P}_1^\pi(\cdot|x) \| \mathcal{P}_2^\pi(\cdot|x)).$$

For a vector-valued function $f : \mathcal{X} \rightarrow \mathbb{R}^d$ (for some $d \geq 1$), we define its mixed p, ∞ -norm as

$$\|f\|_{p,\infty} = \sup_{x \in \mathcal{X}} \|f(x)\|_p.$$

We shall see that the error in gradient depends on the discounted future-state distribution (3). Sometimes we may want to express the errors w.r.t. another distribution $\nu \in \bar{\mathcal{M}}(\mathcal{X})$, which is, for example but not necessarily, the distribution used to collect data to train the model. This requires a change of measure argument. Recall that for a measurable function $f : \mathcal{X} \rightarrow \mathbb{R}$ and two probability measures $\mu_1, \mu_2 \in \bar{\mathcal{M}}(\mathcal{X})$, if μ_1 is absolutely continuous w.r.t. μ_2 ($\mu_1 \ll \mu_2$), the Radon-Nikodym (R-N) derivative $\frac{d\mu_1}{d\mu_2}$ exists, and we have

$$\int f(x) d\mu_1 = \int f(x) \frac{d\mu_1}{d\mu_2} d\mu_2 \leq \left\| \frac{d\mu_1}{d\mu_2} \right\|_{\infty} \int |f(x)| d\mu_2, \quad (13)$$

where

$$\left\| \frac{d\mu_1}{d\mu_2} \right\|_{\infty} = \sup_x \left| \frac{d\mu_1}{d\mu_2}(x) \right|.$$

The supremum of the R-N derivative of ρ_{γ}^{π} w.r.t. ν plays an important role in our results. It is called the Discounted Concentrability Coefficient. We formally define it next.

Definition 1 (Discounted Concentrability Coefficient). *Given two distributions $\rho, \nu \in \bar{\mathcal{M}}(\mathcal{X})$ and a policy π , define*

$$c_{PG}(\rho, \nu; \pi) \triangleq \left\| \frac{d\rho_{\gamma}^{\pi}}{d\nu} \right\|_{\infty}.$$

If the discounted future-state distribution is not absolutely continuous w.r.t. ν , we set $c_{PG}(\rho, \nu; \pi) = \infty$.

The models \mathcal{P}^{π} and $\hat{\mathcal{P}}^{\pi}$ induce discounted future-state distributions ρ_{γ}^{π} and $\hat{\rho}_{\gamma}^{\pi}$. We can compare the expectation of a given (vector-valued) function under these two distributions. The next lemma upper bounds the difference in the ℓ_p -norm of these expectations, and relates it to the error in the models, and some MDP-related quantities.

Lemma 1. *Consider a vector-valued function $f : \mathcal{X} \rightarrow \mathbb{R}^d$, two distributions $\rho, \nu \in \bar{\mathcal{M}}(\mathcal{X})$, and two transition probability kernels \mathcal{P}^{π} and $\hat{\mathcal{P}}^{\pi}$. For any $0 \leq \gamma < 1$, and $1 \leq p \leq \infty$, we have*

$$\left\| \mathbb{E}_{X \sim \rho_{\gamma}(\cdot; \mathcal{P}^{\pi})} [f(X)] - \mathbb{E}_{X \sim \rho_{\gamma}(\cdot; \hat{\mathcal{P}}^{\pi})} [f(X)] \right\|_p \leq \frac{\gamma}{1 - \gamma} \|f\|_{p, \infty} \times \begin{cases} c_{PG}(\rho, \nu; \pi) \|\Delta \mathcal{P}^{\pi}\|_{1, 1(\nu)}, \\ \|\Delta \mathcal{P}^{\pi}\|_{1, \infty}. \end{cases}$$

Proof. For $k = 0, 1, \dots$, define the vector-valued function $E_k : \mathcal{X} \rightarrow \mathbb{R}^d$ by

$$E_k(x) = \int \left(\mathcal{P}^{\pi}(dy|x; k) - \hat{\mathcal{P}}^{\pi}(dy|x; k) \right) f(y),$$

for any $x \in \mathcal{X}$. Note that $E_0(x) = 0$. So we can write

$$\begin{aligned} \frac{1}{1 - \gamma} \int \left(\rho_{\gamma}(dx; \mathcal{P}^{\pi}) - \rho_{\gamma}(dx; \hat{\mathcal{P}}^{\pi}) \right) f(x) &= \sum_{k \geq 0} \gamma^k \int d\rho(x) \left(\mathcal{P}^{\pi}(dy|x; k) - \hat{\mathcal{P}}^{\pi}(dy|x; k) \right) f(y) \\ &= \sum_{k \geq 0} \gamma^k \int d\rho(x) E_k(x). \end{aligned} \quad (14)$$

In order to upper bound the norm of (14), we provide an upper bound on the norm of each E_k . We start by inductively expressing E_k as a function of E_{k-1} , $\Delta\mathcal{P}^\pi$, and other quantities. For $k \geq 1$, and for any $x \in \mathcal{X}$, we write

$$\begin{aligned}
E_k(x) &= \int \left(\mathcal{P}^\pi(dy|x; k) - \hat{\mathcal{P}}^\pi(dy|x; k) \right) f(y) \\
&= \int \left(\mathcal{P}^\pi(dx'|x) \mathcal{P}^\pi(dy|x'; k-1) - \hat{\mathcal{P}}^\pi(dx'|x) \hat{\mathcal{P}}^\pi(dy|x'; k-1) \right) f(y) \\
&= \int \left(\mathcal{P}^\pi(dx'|x) \mathcal{P}^\pi(dy|x'; k-1) - [\mathcal{P}^\pi(dx'|x) - \Delta\mathcal{P}^\pi(dx'|x)] \hat{\mathcal{P}}^\pi(dy|x'; k-1) \right) f(y) \\
&= \int \mathcal{P}^\pi(dx'|x) \left[\mathcal{P}^\pi(dy|x'; k-1) - \hat{\mathcal{P}}^\pi(dy|x'; k-1) \right] f(y) + \Delta\mathcal{P}^\pi(dx'|x) \hat{\mathcal{P}}^\pi(dy|x'; k-1) f(y) \\
&= \int \mathcal{P}^\pi(dx'|x) E_{k-1}(x') + \Delta\mathcal{P}^\pi(dx'|x) \hat{\mathcal{P}}^\pi(dy|x'; k-1) f(y).
\end{aligned}$$

To simplify the notation, we denote the ℓ_p -norm (for any $1 \leq p \leq \infty$) of $E_k(x)$ by $e_k(x)$, i.e., $e_k(x) = \|E_k(x)\|_p$. Moreover, we denote $\varepsilon(x) = \int |\Delta\mathcal{P}^\pi(dx'|x)|$. By the convexity of the ℓ_p -norm for $1 \leq p \leq \infty$ and the application of the Jensen's inequality, we get

$$\begin{aligned}
e_k(x) = \|E_k(x)\|_p &= \left\| \int \mathcal{P}^\pi(dx'|x) E_{k-1}(x') + \Delta\mathcal{P}^\pi(dx'|x) \hat{\mathcal{P}}^\pi(dy|x'; k-1) f(y) \right\|_p \\
&\leq \int \mathcal{P}^\pi(dx'|x) \|E_{k-1}(x')\|_p + \int \left\| \Delta\mathcal{P}^\pi(dx'|x) \hat{\mathcal{P}}^\pi(dy|x'; k-1) f(y) \right\|_p \\
&\leq \int \mathcal{P}^\pi(dx'|x) e_{k-1}(x') + \sup_{y \in \mathcal{X}} \|f(y)\|_p \int |\Delta\mathcal{P}^\pi(dx'|x)| \\
&= \int \mathcal{P}^\pi(dx'|x) e_{k-1}(x') + \|f\|_{p, \infty} \varepsilon(x).
\end{aligned}$$

This relates e_k to e_{k-1} and ε and \mathcal{P}^π . By unrolling e_{k-1}, e_{k-2}, \dots , we get

$$\begin{aligned}
e_k(x) &\leq \|f\|_{p, \infty} \varepsilon(x) + \int \mathcal{P}^\pi(dx'|x) \left[\|f\|_{p, \infty} \varepsilon(x') + \int \mathcal{P}^\pi(dx''|x') e_{k-2}(x'') \right] \leq \dots \\
&\leq \|f\|_{p, \infty} \sum_{i=0}^{k-1} \int \mathcal{P}^\pi(dx'|x; i) \varepsilon(x').
\end{aligned}$$

As a result, the norm of (14) can be upper bounded as

$$\begin{aligned}
\left\| \sum_{k \geq 0} \gamma^k \int d\rho(x) E_k(x) \right\|_p &\leq \sum_{k \geq 0} \gamma^k \int d\rho(x) e_k(x) \\
&\leq \|f\|_{p, \infty} \int d\rho(x) \sum_{k \geq 0} \gamma^k \sum_{i=0}^{k-1} \int \mathcal{P}^\pi(dx'|x; i) \varepsilon(x') \\
&\leq \frac{\gamma}{1-\gamma} \|f\|_{p, \infty} \sum_{k \geq 0} \gamma^k \int d\rho(x) \mathcal{P}^\pi(dx'|x; k) \varepsilon(x') \\
&= \frac{\gamma}{(1-\gamma)^2} \|f\|_{p, \infty} \int \rho_\gamma^\pi(dx) \varepsilon(x), \tag{15}
\end{aligned}$$

where we used the definition of ρ_γ^π (3) in the last equality. By the change of measure argument, we have

$$\int \rho_\gamma^\pi(dx) \varepsilon(x) = \int \frac{d\rho_\gamma^\pi}{d\nu}(x) d\nu(x) \varepsilon(x) \leq \sup_{x \in \mathcal{X}} \frac{d\rho_\gamma^\pi}{d\nu}(x) \int d\nu(x) \varepsilon(x) = c_{PG}(\rho, \nu; \pi) \|\varepsilon\|_{1(\nu)}.$$

By (14) and (15), we get that

$$\left\| \int \left(\rho_\gamma(dx; \mathcal{P}^\pi) - \rho_\gamma(dx; \hat{\mathcal{P}}^\pi) \right) f(x) \right\|_p \leq \frac{\gamma}{1-\gamma} c_{PG}(\rho, \nu; \pi) \|f\|_{p, \infty} \|\varepsilon\|_{1(\nu)}.$$

This leads to the first statement of the lemma.

Alternatively, as $\int \rho_\gamma^\pi(dx') \varepsilon(x') \leq \sup_{x \in \mathcal{X}} \varepsilon(x)$, we can also upper bound (15) by

$$\frac{\gamma}{(1-\gamma)^2} \|f\|_{p, \infty} \|\varepsilon\|_\infty,$$

which leads to the second part of the result. \square

Lemma 1 is for a general function f . By choosing $f(x) = f(x; \theta) = \mathbb{E}_{A \sim \pi_\theta(\cdot|x)} [\nabla_\theta \log \pi_\theta(A|x) Q^{\pi_\theta}(x, A)]$, one can provide an upper bound on the error in the PG (8). To be concrete, we consider a policy from the exponential family.

Suppose that the policy $\pi_\theta : \mathcal{X} \rightarrow \bar{\mathcal{M}}(\mathcal{A})$ is from the exponential family with features $\phi = \phi(a|x) : \mathcal{X} \times \mathcal{A} \rightarrow \mathbb{R}^d$ and parameterized by $\theta \in \Theta \subset \mathbb{R}^d$, and has the density of

$$\pi_\theta(a|x) = \frac{\exp(\phi^\top(a|x)\theta)}{\int \exp(\phi^\top(a'|x)\theta) da'}. \tag{16}$$

If the dependence of π_θ on θ is clear from the context, we may simply refer to it as π .

Theorem 2. Consider the policy parametrization (16), the initial state distribution $\rho \in \bar{\mathcal{M}}(\mathcal{X})$, and the discount factor $0 \leq \gamma < 1$. The policy gradients w.r.t. the true model \mathcal{P}^{π_θ} and the learned model $\hat{\mathcal{P}}^{\pi_\theta}$ are denoted by $\frac{\partial J(\pi_\theta)}{\partial \theta}$ and $\frac{\partial \hat{J}(\pi_\theta)}{\partial \theta}$, respectively (11). Consider an arbitrary distribution $\nu \in \bar{\mathcal{M}}(\mathcal{X})$. Assume that $\|Q^{\pi_\theta}\|_\infty \leq Q_{max}$. For $p \in \{2, \infty\}$, let $B_p = \sup_{(x,a) \in \mathcal{X} \times \mathcal{A}} \|\phi(a|x)\|_p$, and assume that $B_p < \infty$. We have

$$\left\| \frac{\partial J(\pi_\theta)}{\partial \theta} - \frac{\partial \hat{J}(\pi_\theta)}{\partial \theta} \right\|_p \leq \frac{\gamma}{(1-\gamma)^2} Q_{max} B_p \times \begin{cases} c_{PG}(\rho, \nu; \pi_\theta) \|\Delta \mathcal{P}^{\pi_\theta}\|_{1,1(\nu)}, \\ 2 \|\Delta \mathcal{P}^{\pi_\theta}\|_{1, \infty}. \end{cases}$$

Proof. We would like to provide an upper bound on the ℓ_2 and ℓ_∞ norms of $f(x) = f(x; \theta) = \mathbb{E}_{A \sim \pi_\theta(\cdot|x)} [\nabla_\theta \log \pi_\theta(A|x) Q^{\pi_\theta}(x, A)]$, as defined in Lemma 1. For the policy parameterization (16), one can show that

$$\nabla_\theta \log \pi_\theta(a|x) = \phi(a|x) - \mathbb{E}_{A \sim \pi_\theta(\cdot|x)} [\phi(A|x)] = \phi(a|x) - \bar{\phi}(x),$$

with $\bar{\phi}(x) = \bar{\phi}_{\pi_\theta}(x) = \mathbb{E}_{A \sim \pi_\theta(\cdot|x)} [\phi(A|x)]$ being the expected value of the feature $\phi(A|x)$ w.r.t. $\pi_\theta(\cdot|x)$. As $\|Q^{\pi_\theta}\|_\infty \leq Q_{\max}$, for any $1 \leq p \leq \infty$ we have

$$\|f(x; \theta)\|_p \leq \mathbb{E}_{A \sim \pi_\theta(\cdot|x)} \left[\left\| (\phi(A|x) - \bar{\phi}(x)) Q^{\pi_\theta}(x, A) \right\|_p \right] \leq Q_{\max} \mathbb{E}_{A \sim \pi_\theta(\cdot|x)} \left[\left\| \phi(A|x) - \bar{\phi}(x) \right\|_p \right]. \quad (17)$$

Let us focus on $p = 2$. We have

$$\begin{aligned} \mathbb{E}_{A \sim \pi_\theta(\cdot|x)} \left[\left\| \phi(A|x) - \bar{\phi}(x) \right\|_2 \right] &\leq \sqrt{\mathbb{E}_{A \sim \pi_\theta(\cdot|x)} \left[\left\| \phi(A|x) - \bar{\phi}(x) \right\|_2^2 \right]} \\ &= \sqrt{\mathbb{E}_{A \sim \pi_\theta(\cdot|x)} \left[\sum_{i=1}^d |\phi_i(A|x) - \bar{\phi}_i(x)|^2 \right]} \\ &= \sqrt{\sum_{i=1}^d \text{Var}_{A \sim \pi_\theta(\cdot|x)} [\phi_i(A|x)]} \\ &\leq \sqrt{\sum_{i=1}^d \mathbb{E}_{A \sim \pi_\theta(\cdot|x)} [\phi_i^2(A|x)]} \\ &= \sqrt{\mathbb{E}_{A \sim \pi_\theta(\cdot|x)} \left[\sum_{i=1}^d \phi_i^2(A|x) \right]} = \sqrt{\mathbb{E}_{A \sim \pi_\theta(\cdot|x)} \left[\left\| \phi(A|x) \right\|_2^2 \right]} \leq B_2. \end{aligned}$$

Therefore by (17),

$$\|f(x; \theta)\|_2 \leq Q_{\max} B_2. \quad (18)$$

For $p = \infty$, we have

$$\mathbb{E}_{A \sim \pi_\theta(\cdot|x)} \left[\left\| \phi(A|x) - \bar{\phi}(x) \right\|_\infty \right] \leq \mathbb{E}_{A \sim \pi_\theta(\cdot|x)} \left[\left\| \phi(A|x) \right\|_\infty + \left\| \bar{\phi}(x) \right\|_\infty \right] \leq B_\infty + \left\| \bar{\phi}(x) \right\|_\infty.$$

We also have $\left\| \bar{\phi}(x) \right\|_\infty = \left\| \mathbb{E}_{A \sim \pi_\theta(\cdot|x)} [\phi(A|x)] \right\|_\infty \leq \mathbb{E}_{A \sim \pi_\theta(\cdot|x)} \left[\left\| \phi(A|x) \right\|_\infty \right] \leq B_\infty$. These together with (17) show that

$$\|f(x; \theta)\|_2 \leq 2Q_{\max} B_\infty. \quad (19)$$

Noticing that $\frac{\partial J(\pi_\theta)}{\partial \theta} = \frac{1}{1-\gamma} \mathbb{E}_{X \sim \rho_\gamma(\cdot; \mathcal{P}^\pi)} [f(X)]$ with the choice of f in this proof (and similar for $\frac{\partial \hat{J}(\pi_\theta)}{\partial \theta}$), we can apply Lemma 1 using upper bounds (18) and (19) to obtain the desired result. \square

This theorem shows the effect of the model error, quantified in the total variation-based norms $\|\Delta\mathcal{P}^{\pi_\theta}\|_{1,\infty}$ or $\|\Delta\mathcal{P}^{\pi_\theta}\|_{1,1(\nu)}$, on the PG estimate. The norms measure how different the distribution of the true dynamics $\mathcal{P}^{\pi_\theta} = \mathcal{P}^{*\pi_\theta}$ is from the distribution of the estimate $\hat{\mathcal{P}}^{\pi_\theta}$, according to the difference in the total variation distance between their next-state distributions, i.e., $\|\mathcal{P}^{\pi_\theta}(\cdot|x) - \hat{\mathcal{P}}^{\pi_\theta}(\cdot|x)\|_1$. The difference between them is on whether we take the supremum over the state space \mathcal{X} or average (according to ν) over it. Clearly, $\|\Delta\mathcal{P}^{\pi_\theta}\|_{1,\infty}$ is a more strict norm compared to $\|\Delta\mathcal{P}^{\pi_\theta}\|_{1,1(\nu)}$.

For the average norm, a concentrability coefficient $c_{\text{PG}}(\rho, \nu; \pi_\theta)$ appears in the bound. This coefficient measures how different the discounted future-state distribution $\rho_\gamma^{\pi_\theta}$ is from the distribution ν , used for taking average over the total variation errors. If ν is selected to be $\rho_\gamma^{\pi_\theta}$, the coefficient $c_{\text{PG}}(\rho, \nu; \pi_\theta)$ would be equal to 1. Moreover, if we choose ν to be equal to the initial state distribution ρ , one can show that the coefficient $c_{\text{PG}}(\rho, \rho; \pi_\theta) \leq \frac{1}{1-\gamma}$ (we show this in the proof of Theorem 3).

We can use this upper bound to relate the quality of an MLE to the quality of the PGs. By Pinsker's inequality, the TV distance of two distributions can be upper bounded by their KL-divergence:

$$\|\Delta\mathcal{P}^{\pi_\theta}(\cdot|x)\|_1 \leq \sqrt{2\text{KL}\left(\mathcal{P}^{\pi_\theta}(\cdot|x)\|\hat{\mathcal{P}}_{\pi_\theta}(\cdot|x)\right)}.$$

Therefore, we also have $\|\Delta\mathcal{P}^{\pi_\theta}\|_{1,\infty} \leq \sqrt{2\text{KL}_\infty(\mathcal{P}^{\pi_\theta}\|\hat{\mathcal{P}}_{\pi_\theta})}$ too. Moreover, as

$$\begin{aligned} \mathbb{E}_\nu [\|\Delta\mathcal{P}^{\pi_\theta}(\cdot|X)\|_1]^2 &\leq \mathbb{E}_\nu \left[\|\Delta\mathcal{P}^{\pi_\theta}(\cdot|X)\|_1^2 \right] \leq \mathbb{E}_\nu \left[2\text{KL}\left(\mathcal{P}^{\pi_\theta}(\cdot|X)\|\hat{\mathcal{P}}_{\pi_\theta}(\cdot|X)\right) \right] \\ &= 2\text{KL}_{1(\nu)}\left(\mathcal{P}^{\pi_\theta}\|\hat{\mathcal{P}}_{\pi_\theta}\right), \end{aligned}$$

we get $\|\Delta\mathcal{P}^{\pi_\theta}\|_{1,1(\nu)} \leq \sqrt{2\text{KL}_{1(\nu)}(\mathcal{P}^{\pi_\theta}\|\hat{\mathcal{P}}_{\pi_\theta})}$. Combined with the upper bound of Theorem 2, we get that

$$\left\| \nabla_\theta J(\pi_\theta) - \nabla_\theta \hat{J}(\pi_\theta) \right\|_p \leq \frac{\gamma}{(1-\gamma)^2} Q_{\max} B_p \times \begin{cases} c_{\text{PG}}(\rho, \nu; \pi_\theta) \sqrt{2\text{KL}_{1(\nu)}(\mathcal{P}^{\pi_\theta}\|\hat{\mathcal{P}}_{\pi_\theta})}, \\ 2\sqrt{2\text{KL}_\infty(\mathcal{P}^{\pi_\theta}\|\hat{\mathcal{P}}_{\pi_\theta})}. \end{cases} \quad (20)$$

This is an upper bound on the PG error for conventional model learning procedures. Recall that the MLE is the minimizer of the KL-divergence between the empirical distribution of samples generated from \mathcal{P}^{π_θ} and $\hat{\mathcal{P}}^{\pi_\theta}$. There would be some statistical deviation between its minimizer and the minimizer of $\min_{\mathcal{P} \in \mathcal{M}} \text{KL}(\mathcal{P}^{\pi_\theta}\|\mathcal{P})$, but if the model space is chosen properly, the difference between the minimizer decreases as the number of samples increases.

This upper bound also suggests why PAML might be a more suitable approach in learning a model. An MLE-based approach tries to minimize an upper bound of an upper bound for the quantity that we care about (PG error). This consecutive upper bounding might be quite loose. On the other hand, the population version of PAML's loss (8) is exactly the error in the PG estimates that we care about.

This upper bound suggests why PAML might be a more suitable approach in learning a model. An MLE-based approach tries to minimize an upper bound of an upper bound for the quantity that we care about (PG error). This consecutive upper bounding might be quite loose. On the other hand, the population version of PAML's loss (8) is exactly the error in the PG estimates

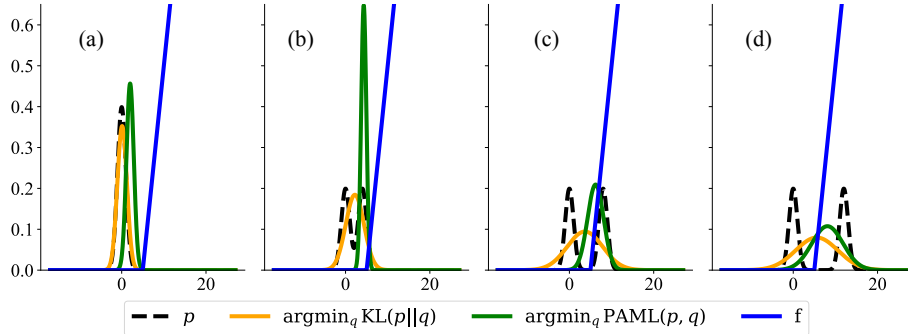


Figure 1: Visualization of minimizing models for PAML and MLE. \mathcal{P}^* , denoted p , is a Gaussian mixture model and the learned model q that is a single Gaussian. The loss minimized by PAML for this simple case is: $|\sum_x (\mathcal{P}^* - \hat{\mathcal{P}}) f(x)|^2$.

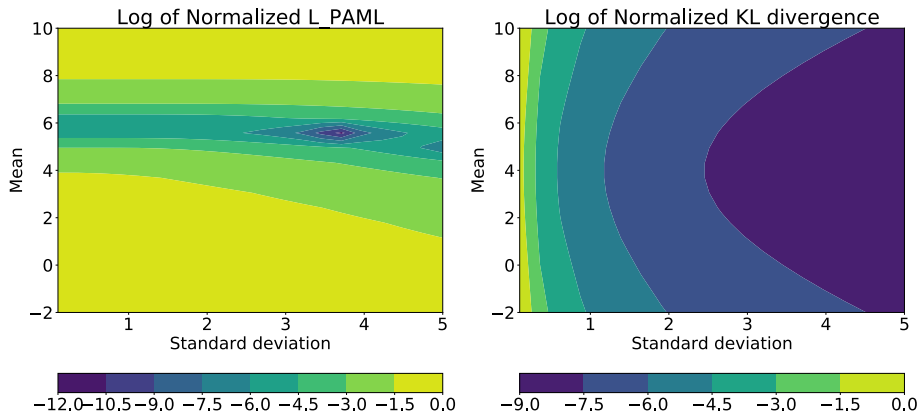


Figure 2: Contours of the two loss surfaces for case (c) above, demonstrating the locations of the minimizers for each. Note that the losses were log-normalized for better visual contrast in this figure.

that we care about. A question that may arise is that although these two losses are different, are their minimizers the same? In Figures 1 and 2 we show through a simple visualization that the minimizers of PAML and KL could indeed be different.

4.2 Convergence of Model-Based PG

We provide a convergence guarantee for a MBPG method. The guarantee applies for the restricted policy space, and shows that the obtained policy is not much worse than the best policy in the class. The error depends on the number of PG iterations, the error in the PG computation, and some other properties of the MDP and the sampling distributions. The analysis is for when the PG can be calculated exactly, i.e., we do not analyze the error caused by sampling.

Until recently, there had not been much theoretical work on the convergence of the PG algorithm, beyond proving its convergence to a local optimum. There has been a recent surge of interest in

providing global convergence guarantees for PG methods and variants (Agarwal et al., 2019; Shani et al., 2019; Bhandari & Russo, 2019; Liu et al., 2019). This section is based on the recent work by Agarwal et al. (2019), who have provided convergence results for several variations of the PG method. Their result is for a model-free setting, where the gradients are computed according to the true dynamics \mathcal{P}^π of the policy. We modify their result to show the convergence of MBPG. In addition to this difference, we introduce a new notion of policy approximation error, which is perhaps a better characterization of the approximation error of the policy space.

Instead of extending their result to be suitable for the model-based setting, we provide a slightly, but crucially, different result for the convergence of a PG algorithm. In particular, we consider the same setting as in Section 6.2 (Projected Policy Gradient for Constrained Policy Classes) of Agarwal et al. (2019) and prove a result similar to their Theorem 6.11. We briefly mention that the main difference with their result is that our policy approximation error, to be defined shortly, considers **1**) how well one can approximate the best policy in the policy class Π , instead of the greedy policy w.r.t. the action-value function of the current policy, in their result, and **2**) the interaction of the value function and the policy, as opposed to the error in only approximating the policy in their result. We explain this in more detail after we describe all the relevant quantities. This result, in turn, can be used to prove a convergence guarantee, as in their Corollary 6.14. Before continuing, we mention that we liberally use the groundwork provided by Agarwal et al. (2019).

We analyze a projected PG with the assumption that the PGs are computed exactly. We consider a setup where the performance is evaluated according to a distribution $\rho \in \mathcal{M}(\mathcal{X})$, but the PG is computed according to a possibly different distribution $\mu \in \mathcal{M}(\mathcal{X})$. To be concrete, let us consider a policy space $\Pi = \{\pi_\theta : \theta \in \Theta\}$ with Θ being a convex subset of \mathbb{R}^d and Proj_Θ be the projection operator onto Θ . Consider the projected policy gradient procedure

$$\theta_{t+1} \leftarrow \text{Proj}_\Theta [\theta_t + \eta \nabla_\theta J_\mu(\pi_{\theta_t})],$$

with a learning rate $\eta > 0$, to be specified. A policy π_θ is called ε -stationary if for all $\theta + \delta \in \Theta$ and with the constraint that $\|\delta\|_2 \leq 1$, we have

$$\delta^\top \nabla_\theta J_\mu(\pi_\theta) \leq \varepsilon. \quad (21)$$

Let us denote the best policy in the policy class Π according to the initial distribution ρ by $\bar{\pi}_\rho$ (or simply $\bar{\pi}$, if it is clear from the context), i.e.,

$$\bar{\pi} \leftarrow \underset{\pi \in \Pi}{\text{argmax}} J_\rho(\pi). \quad (22)$$

Let us denote the best policy in the policy class Π according to the initial distribution ρ by $\bar{\pi}_\rho$ (or simply $\bar{\pi}$, if it is clear from the context), i.e., $\bar{\pi} \leftarrow \underset{\pi \in \Pi}{\text{argmax}} J_\rho(\pi)$. We define a function that we call it *Policy Approximation Error (PAE)*. Given a policy parameter θ and $w \in \mathbb{R}^d$, and for a probability distribution $\nu \in \bar{\mathcal{M}}(\mathcal{X})$, define

$$L_{\text{PAE}}(\theta, w; \nu) \triangleq \mathbb{E}_{X \sim \nu} \left[\left\| \sum_{a \in \mathcal{A}} (\bar{\pi}(a|X) - \pi_\theta(a|X) - w^\top \nabla_\theta \pi_\theta(a|X)) Q^{\pi_\theta}(X, a) \right\|^2 \right].$$

This can be roughly interpreted as the error in approximating the improvement in the value from the current policy π_θ to the best policy in the class, $\bar{\pi}$, i.e., $\sum_{a \in \mathcal{A}} (\bar{\pi}(a|X) - \pi_\theta(a|X)) Q^{\pi_\theta}(X, a)$, by a linear model $\sum_{a \in \mathcal{A}} w^\top \nabla_\theta \pi_\theta(a|X) Q^{\pi_\theta}(X, a) = w^\top \mathbb{E}_{A \sim \pi_\theta(\cdot|X)} [\nabla_\theta \log \pi_\theta(a|X) Q^{\pi_\theta}(X, a)]$.

For any $\theta \in \Theta$, we can define the best $w^*(\theta) = w^*(\theta; \nu)$ that minimizes $L_{\text{PAE}}(\theta, w; \nu)$ as

$$w^*(\theta; \nu) \leftarrow \underset{w+\theta \in \Theta}{\operatorname{argmin}} L_{\text{PAE}}(\theta, w; \nu). \quad (23)$$

We use $L_{\text{PAE}}(\theta; \nu)$ to represent $L_{\text{PAE}}(\theta, w^*(\theta); \nu)$. We may drop the distribution ν whenever it is clear from the context.

The following result relates the performance loss of a policy compared to the best policy in the class (i.e., $J_\rho(\bar{\pi}) - J_\rho(\pi_\theta)$) to its ε -stationarity, the policy approximation error, and some other quantities. As we shall see, one can show the ε -stationarity of projected PG using tools from the optimization literature (e.g., Theorem 10.15 of [Beck 2017](#)), hence providing a performance guarantee.

Theorem 3. *Consider any initial distributions $\rho, \mu \in \bar{\mathcal{M}}(\mathcal{X})$ and a policy π_θ with $\theta \in \Theta$, a convex set. Suppose that π_θ is an ε -stationary w.r.t. distribution μ (21). Let $\bar{\pi}$ be defined as (22) and $w^*(\theta; \rho_\gamma^{\bar{\pi}})$ as (23). Assume that $\rho_\gamma^{\bar{\pi}}$ is absolutely continuous w.r.t. μ , and $0 \leq \gamma < 1$. We then have*

$$J_\rho(\bar{\pi}) - J_\rho(\pi_\theta) \leq \frac{1}{1-\gamma} \left[L_{\text{PAE}}(\theta; \rho_\gamma^{\bar{\pi}}) + \left\| \frac{d\rho_\gamma^{\bar{\pi}}}{d\mu} \right\|_\infty (1 \vee \|w^*(\theta; \rho_\gamma^{\bar{\pi}})\|) \varepsilon \right].$$

Proof. By the performance difference lemma (Lemma 6.1 of [Kakade & Langford \(2002\)](#) or Lemma 3.2 of [Agarwal et al. 2019](#)) for any policy π_θ and the best policy in class $\bar{\pi} = \bar{\pi}_\rho$, we have that

$$\begin{aligned} J_\rho(\bar{\pi}) - J_\rho(\pi_\theta) &= \frac{1}{1-\gamma} \mathbb{E}_{X \sim \rho_\gamma^{\bar{\pi}}} \left[\sum_{a \in \mathcal{A}} \bar{\pi}(a|X) A^{\pi_\theta}(X, a) \right] \\ &\stackrel{(a)}{=} \frac{1}{1-\gamma} \mathbb{E}_{X \sim \rho_\gamma^{\bar{\pi}}} \left[\sum_{a \in \mathcal{A}} (\bar{\pi}(a|X) - \pi_\theta(a|X)) A^{\pi_\theta}(X, a) \right] \\ &= \frac{1}{1-\gamma} \mathbb{E}_{X \sim \rho_\gamma^{\bar{\pi}}} \left[\sum_{a \in \mathcal{A}} (\bar{\pi}(a|X) - \pi_\theta(a|X)) (Q^{\pi_\theta}(X, a) - V^{\pi_\theta}(X)) \right] \\ &\stackrel{(b)}{=} \frac{1}{1-\gamma} \mathbb{E}_{X \sim \rho_\gamma^{\bar{\pi}}} \left[\sum_{a \in \mathcal{A}} (\bar{\pi}(a|X) - \pi_\theta(a|X)) Q^{\pi_\theta}(X, a) \right], \end{aligned}$$

where (a) is because $\sum_a \pi_\theta(a|x) A^{\pi_\theta}(x, a) = \sum_a \pi_\theta(a|x) (Q^{\pi_\theta}(x, a) - V^{\pi_\theta}(x)) = 0$ by the definition of the state-value function, and (b) is because $\sum_a (\bar{\pi}(a|x) - \pi_\theta(a|x)) V^{\pi_\theta}(x) = V^{\pi_\theta}(x) \sum_a \bar{\pi}(a|x) - \pi_\theta(a|x) = V^{\pi_\theta}(x) (1 - 1) = 0$.

Let $w \in \mathbb{R}^d$ be an arbitrary vector. By adding and subtracting the scalar $w^\top \nabla_\theta \pi_\theta Q^{\pi_\theta}(X, a)$, we obtain

$$\begin{aligned} J_\rho(\bar{\pi}) - J_\rho(\pi_\theta) &= \frac{1}{1-\gamma} \mathbb{E}_{X \sim \rho_\gamma^{\bar{\pi}}} \left[\sum_{a \in \mathcal{A}} (\bar{\pi}(a|X) - \pi_\theta(a|X) - w^\top \nabla_\theta \pi_\theta) Q^{\pi_\theta}(X, a) \right] + \\ &\quad \frac{1}{1-\gamma} \mathbb{E}_{X \sim \rho_\gamma^{\bar{\pi}}} \left[\sum_{a \in \mathcal{A}} w^\top \nabla_\theta \pi_\theta(a|X) Q^{\pi_\theta}(X, a) \right] \\ &\leq \frac{1}{1-\gamma} L_{\text{PAE}}(\theta, w; \rho_\gamma^{\bar{\pi}}) + w^\top \frac{1}{1-\gamma} \mathbb{E}_{X \sim \rho_\gamma^{\bar{\pi}}} \left[\sum_{a \in \mathcal{A}} \pi_\theta(a|X) \nabla_\theta \log \pi_\theta(a|X) Q^{\pi_\theta}(X, a) \right]. \end{aligned}$$

We make two observations. The first is that as this inequality holds for any w , it holds for $w^*(\theta)$ too, so we can substitute $L_{\text{PAE}}(\theta, w; \rho_\gamma^\pi)$ with $L_{\text{PAE}}(\theta; \rho_\gamma^\pi) = L_{\text{PAE}}(\theta, w^*(\theta); \rho_\gamma^\pi)$. The second is that the expectation $\mathbb{E}_{X \sim \rho_\gamma^\pi} [\sum_{a \in \mathcal{A}} \pi_\theta(a|X) \nabla_\theta \log \pi_\theta(a|X) Q^{\pi_\theta}(X, a)]$ is of the same general form of a policy gradient $\nabla_\theta J(\pi_\theta)$, with the difference that the state distribution is w.r.t. the discounted future-state distribution of starting from ρ and following the best policy in class $\bar{\pi}$, as opposed to the discounted future-state distribution of starting from μ and following policy π_θ , cf. (11). We use a change of measure argument, similar to (13), to convert the expectation to the desired form. Based on these two observations, we obtain

$$J_\rho(\bar{\pi}) - J_\rho(\pi_\theta) \leq \frac{1}{1-\gamma} L_{\text{PAE}}(\theta; \rho_\gamma^\pi) + \left\| \frac{d\rho_\gamma^\pi}{d\mu_\gamma^{\pi_\theta}} \right\|_\infty w^*(\theta)^\top \nabla_\theta J_\mu(\pi_\theta). \quad (24)$$

We would like to use the ε -stationary of the policy in order to upper bound the right-hand side (RHS). Define $\delta = \frac{w^*(\theta)}{1 \vee \|w^*(\theta)\|}$. It is clear that $\|\delta\| \leq 1$. As both θ and $\theta + w^*(\theta)$ belong to the set Θ and Θ is convex, the line segment connecting them is within Θ too. The point $\theta + \delta$ is on that line segment, so it is within Θ . By the ε -stationarity, we obtain that

$$w^*(\theta)^\top \nabla_\theta J_\mu(\pi_\theta) = (1 \vee \|w^*(\theta)\|) \delta^\top \nabla_\theta J_\mu(\pi_\theta) \leq (1 \vee \|w^*(\theta)\|) \varepsilon.$$

We plug-in this result in (24) to get

$$\begin{aligned} J_\rho(\bar{\pi}) - J_\rho(\pi_\theta) &\leq \frac{1}{1-\gamma} L_{\text{PAE}}(\theta; \rho_\gamma^\pi) + \left\| \frac{d\rho_\gamma^\pi}{d\mu_\gamma^{\pi_\theta}} \right\|_\infty (1 \vee \|w^*(\theta)\|) \varepsilon \\ &\leq \frac{1}{1-\gamma} \left[L_{\text{PAE}}(\theta; \rho_\gamma^\pi) + \left\| \frac{d\rho_\gamma^\pi}{d\mu} \right\|_\infty (1 \vee \|w^*(\theta)\|) \varepsilon \right]. \end{aligned}$$

The second inequality is because of the property of the Radon-Nikodym derivative that states that if $\rho_\gamma^\pi \ll \mu \ll \mu_\gamma^{\pi_\theta}$, we have

$$\frac{d\rho_\gamma^\pi}{d\mu_\gamma^{\pi_\theta}} = \frac{d\rho_\gamma^\pi}{d\mu} \frac{d\mu}{d\mu_\gamma^{\pi_\theta}},$$

and the fact that $\left\| \frac{d\mu}{d\mu_\gamma^{\pi_\theta}} \right\|_\infty \leq \frac{1}{1-\gamma}$. To see the truth of the latter claim, consider any measurable set $\mathcal{X}_0 \subset \mathcal{X}$ and any policy π . The probability of \mathcal{X}_0 according to μ_γ^π is greater or equal to $(1-\gamma)$ times of its probability according to μ , that is, $\mu_\gamma^\pi(\mathcal{X}_0) = (1-\gamma)[\mu(\mathcal{X}_0) + (\mu \mathcal{P}^\pi)(\mathcal{X}_0) + (\mu \mathcal{P}^\pi)^2(\mathcal{X}_0) + \dots] \geq (1-\gamma)\mu(\mathcal{X}_0)$.

To verify the conditions $\rho_\gamma^\pi \ll \mu \ll \mu_\gamma^{\pi_\theta}$, notice that the condition $\rho_\gamma^\pi \ll \mu$ is satisfied by assumption; the condition $\mu \ll \mu_\gamma^{\pi_\theta}$ is satisfied as we just show that $\mu_\gamma^\pi(\mathcal{X}_0) \geq (1-\gamma)\mu(\mathcal{X}_0)$ for any policy; and if $\rho_\gamma^\pi \ll \mu$ is satisfied, $\rho_\gamma^\pi \ll \mu_\gamma^{\pi_\theta}$ is satisfied too. \square

This result is similar to Theorem 6.11 of Agarwal et al. (2019). The difference is in the policy approximation error term. Instead of $L_{\text{PAE}}(\theta, w; \nu)$, they have a term called *Bellman Policy Error*, which is defined as

$$L_{\text{BPE}}(\theta, w; \nu) \triangleq \mathbb{E}_{X \sim \nu} \left[\sum_{a \in \mathcal{A}} \left| \operatorname{argmax}_{a \in \mathcal{A}} Q^{\pi_\theta}(X, a) - \pi_\theta(a|X) - w^\top \nabla_\theta \pi_\theta(a|X) \right| \right].$$

The minimizer of this function over w , that is $L_{\text{BPE}}(\theta, \rho_\gamma^\pi) = \min_{w+\theta \in \Theta} L_{\text{BPE}}(\theta, w; \rho_\gamma^\pi)$, appears instead of $L_{\text{PAE}}(\theta; \rho_\gamma^\pi)$ in the upper bound of Theorem 3. The Bellman Policy Error measures the error in approximating the 1-step greedy policy improvement relative to a policy in the class.

It is a curious question to know which of L_{BPE} and L_{PAE} is a better characterizer of the policy approximation error. We do not have a definite answer to this question so far, but we make two observations that show that L_{PAE} is better (smaller) at least in some circumstances.

The first observation is that L_{BPE} ignores the value function Q^π and its interaction with the policy error, whereas L_{PAE} does not. As an example, if the reward function is constant everywhere, the action-value function Q^π for any policy would be constant too. In this case, $L_{\text{PAE}}(\theta; \nu)$ is zero (simply choose $w = 0$ as the minimizer), but L_{BPE} may not be.

Weighting the error in policies with a value function is reminiscent of the loss function appearing in some classification-based approximate policy iteration methods such as the work by [Lazarcic et al. \(2010\)](#); [Farahmand et al. \(2015\)](#); [Lazarcic et al. \(2016\)](#) (and different from the original formulation by [Lagoudakis & Parr \(2003b\)](#) and more recent instantiation by [Silver et al. \(2017a\)](#) whose policy loss does not incorporate the value functions), Policy Search by Dynamic Programming ([Bagnell et al., 2004](#)), and Conservative Policy Iteration ([Kakade & Langford, 2002](#)).

The other observation is that if the policy is parameterized so that there is only one policy in the policy class $\Pi = \{\pi_\theta : \theta \in \Theta\}$ (but still Θ is a subset of \mathbb{R}^d , so we can define PG), any policy $\pi_\theta \in \Pi$ is the same as the best policy $\bar{\pi}$, i.e., $\pi_\theta = \bar{\pi}$. In that case, $L_{\text{PAE}}(\theta, 0; \nu) = \mathbb{E}_{X \sim \nu} [|\sum_{a \in \mathcal{A}} (\bar{\pi}(a|X) - \bar{\pi}(a|X) - 0^\top \nabla_\theta \pi_\theta(a|X)) Q^{\bar{\pi}}(X, a)|] = 0$. On the other hand, it may not be possible to make $L_{\text{BPE}}(\theta, w; \nu) = \mathbb{E}_{X \sim \nu} [\sum_{a \in \mathcal{A}} |\arg\max_{a \in \mathcal{A}} Q^{\bar{\pi}}(X, a) - \bar{\pi}(a|X) - w^\top \nabla_\theta \pi_\theta(a|X)|]$ equal to zero for any choice of w , as it requires the policy space to approximate the greedy policy, which is possibly outside the policy space. We leave further study of these two policy approximation errors to a future work.

To provide a convergence rate, we require some extra assumptions on the smoothness of the policy.

Assumption A1 (Assumption 6.12 of [Agarwal et al. \(2019\)](#)) Assume that there exist finite constants $\beta_1, \beta_2 \geq 0$ such that for all $\theta_1, \theta_2 \in \Theta$, and for all $(x, a) \in \mathcal{X} \times \mathcal{A}$, we have

$$\begin{aligned} |\pi_{\theta_1}(a|x) - \pi_{\theta_2}(a|x)| &\leq \beta_1 \|\theta_1 - \theta_2\|_2, \\ \|\nabla_\theta \pi_{\theta_1}(a|x) - \nabla_\theta \pi_{\theta_2}(a|x)\|_2 &\leq \beta_2 \|\theta_1 - \theta_2\|_2. \end{aligned}$$

[Agarwal et al. \(2019\)](#) assume that the reward function is in $[0, 1]$. Here we consider the reward to be R_{\max} -bounded, which leads to having the value function being Q_{\max} -bounded with $Q_{\max} = \frac{R_{\max}}{1-\gamma}$. Some results should be slightly modified (particularly, Lemma E.2 and E.5 of that paper). We report the modifications in Appendix A.2. Here we just mention that the difference is that the upper bounds in those result should be multiplied by $(1 - \gamma)Q_{\max}$.

We are ready to analyze the convergence behaviour of a model-based PG algorithm. We consider a projected PG algorithm that uses the model $\hat{\mathcal{P}}^{\pi_{\theta_k}}$ to compute the gradient, i.e.,

$$\theta_{t+1} \leftarrow \text{Proj}_\Theta \left[\theta_t + \eta \nabla_\theta \hat{J}_\mu(\theta_k) \right], \quad (25)$$

with a learning rate $\eta > 0$ to be specified.

Theorem 4. Consider any initial distributions $\rho, \mu \in \bar{\mathcal{M}}(\mathcal{X})$ and a policy space Π parameterized by $\theta \in \Theta$ with Θ being a convex subset of \mathbb{R}^d . Assume that all policies $\pi_\theta \in \Pi$ satisfy Assumption A1. Furthermore, suppose that the value function is bounded by Q_{\max} , the MDP has a finite number of actions $|\mathcal{A}|$, and $0 \leq \gamma < 1$. Let

$$\beta = Q_{\max} \left[\frac{2\gamma\beta_1^2|\mathcal{A}|^2}{(1-\gamma)^2} + \frac{\beta_2|\mathcal{A}|}{1-\gamma} \right]. \quad (26)$$

Let T be an integer number. Starting from a $\pi_{\theta_0} \in \Pi$, consider the sequence of policies $\pi_{\theta_1}, \dots, \pi_{\theta_T}$ generated by the projected model-based PG algorithm (25) with step-size $\eta = \frac{1}{\beta}$. Let $W = \sup_{\theta \in \Theta} \|w^*(\theta; \rho_{\gamma}^{\bar{\pi}})\|_2$, and assume that $W < \infty$. Assume that for any policy $\pi_{\theta} \in \{\pi_{\theta_0}, \dots, \pi_{\theta_{T-1}}\}$, there exists a constant ε_{model} such that the policy gradient according to the model $\hat{\mathcal{P}}^{\pi_{\theta}}$ satisfies

$$\left\| \nabla_{\theta} J_{\mu}(\pi_{\theta}) - \nabla_{\theta} \hat{J}_{\mu}(\pi_{\theta}) \right\|_2 \leq \varepsilon_{model}.$$

We then have

$$\min_{t=0, \dots, T} J_{\rho}(\bar{\pi}) - J_{\rho}(\pi_{\theta_t}) \leq \frac{1}{1-\gamma} \left[\sup_{\theta \in \Theta} L_{PAE}(\theta; \rho_{\gamma}^{\bar{\pi}}) + \left\| \frac{d\rho_{\gamma}^{\bar{\pi}}}{d\mu} \right\|_{\infty} (1 \vee W) \left(4\sqrt{\frac{Q_{\max}\beta}{T}} + \varepsilon_{model} \right) \right].$$

Proof. By Lemma 6 in Appendix A.2, $V^{\pi_{\theta}}$ is β -smooth for all states x with β specified in (26). Hence $\hat{J}_{\mu}(\pi_{\theta})$ is also β -smooth.

Let the gradient mapping for θ be defined as

$$G^{\eta}(\theta) = \frac{1}{\eta} \left(\text{Proj}_{\Theta} \left[\theta + \eta \nabla_{\theta} \hat{J}_{\mu} \right] - \theta \right).$$

For a projected gradient ascent on a β -smooth function over a convex set with a step-size of $\eta = \frac{1}{\beta}$, Theorem 10.15 of Beck (2017) shows that

$$\min_{t=0, \dots, T-1} \|G^{\eta}(\theta_t)\|_2 \leq \sqrt{\frac{2\beta \left(\hat{J}_{\mu}(\pi^*) - \hat{J}_{\mu}(\pi_{\theta_0}) \right)}{T}} \leq \sqrt{\frac{4Q_{\max}\beta}{T}}. \quad (27)$$

By Proposition 7 in Appendix A.2 (originally Proposition D.1 of Agarwal et al. 2019) if we let $\theta' = \theta + \eta G^{\eta}$, we have that

$$\max_{\theta + \delta \in \Theta, \|\delta\|_2 \leq 1} \delta^{\top} \nabla_{\theta} \hat{J}_{\mu}(\pi_{\theta'}) \leq (\eta\beta + 1) \|G^{\eta}(\theta)\|_2.$$

This upper bound along (27) and $\beta\eta + 1 = 2$ show that the sequence $\theta_0, \theta_1, \dots, \theta_T$ generated by (25) satisfies

$$\min_{t=0, \dots, T} \max_{\theta_t + \delta \in \Theta, \|\delta\|_2 \leq 1} \delta^{\top} \nabla_{\theta} \hat{J}_{\mu}(\pi_{\theta_t}) \leq (\eta\beta + 1) \min_{t=0, \dots, T-1} \|G^{\eta}(\theta_t)\|_2 \leq 4\sqrt{\frac{Q_{\max}\beta}{T}}. \quad (28)$$

Note that this is a guarantee on $\delta^{\top} \nabla_{\theta} \hat{J}_{\mu}(\pi_{\theta_t})$, the inner product of a direction δ with the PG according to $\hat{\mathcal{P}}^{\pi}$, and not $\delta^{\top} \nabla_{\theta} J_{\mu}(\pi_{\theta_t})$, which has the PG according to \mathcal{P}^{π} and is what we need in order to compare the performance. For any θ , including $\theta_0, \theta_1, \dots, \theta_T$, we have

$$\begin{aligned} \max_{\|\delta\|_2 \leq 1} |\delta^{\top} \nabla_{\theta} J_{\mu}(\pi_{\theta})| &= \max_{\|\delta\|_2 \leq 1} \left| \delta^{\top} \left(\nabla_{\theta} J_{\mu}(\pi_{\theta}) - \nabla_{\theta} \hat{J}_{\mu}(\pi_{\theta}) + \nabla_{\theta} \hat{J}_{\mu}(\pi_{\theta}) \right) \right| \\ &\leq \max_{\|\delta\|_2 \leq 1} \left| \delta^{\top} \nabla_{\theta} \hat{J}_{\mu}(\pi_{\theta}) \right| + \max_{\|\delta\|_2 \leq 1} \left| \delta^{\top} \left(\nabla_{\theta} J_{\mu}(\pi_{\theta}) - \nabla_{\theta} \hat{J}_{\mu}(\pi_{\theta}) \right) \right| \\ &= \max_{\|\delta\|_2 \leq 1} \left| \delta^{\top} \nabla_{\theta} \hat{J}_{\mu}(\pi_{\theta}) \right| + \left\| \nabla_{\theta} J_{\mu}(\pi_{\theta}) - \nabla_{\theta} \hat{J}_{\mu}(\pi_{\theta}) \right\|_2. \end{aligned} \quad (29)$$

This inequality together with (28) provide an upper bound on the ε -stationarity of

$$\min_{t=0,\dots,T} \max_{\|\delta\|_2 \leq 1} |\delta^\top \nabla_\theta J_\mu(\pi_{\theta_t})|.$$

We can now evoke Theorem 3. By the assumption that $\|\nabla_\theta J_\mu(\pi_{\theta_t}) - \nabla_\theta \hat{J}_\mu(\pi_{\theta_t})\|_2 \leq \varepsilon_{\text{model}}$ and $W = \sup_{\theta \in \Theta} \|w^*(\theta; \rho_\gamma^\pi)\|_2$, we get that

$$\begin{aligned} \min_{t=0,\dots,T} J_\rho(\bar{\pi}) - J_\rho(\pi_{\theta_t}) &\leq \frac{1}{1-\gamma} \min_{t=0,\dots,T} \left[L_{\text{PAE}}(\theta_t; \rho_\gamma^\pi) + \left\| \frac{d\rho_\gamma^\pi}{d\mu} \right\|_\infty (1 \vee \|w^*(\theta_t; \rho_\gamma^\pi)\|) \max_{\|\delta\|_2 \leq 1} |\delta^\top \nabla_\theta J_\mu(\pi_{\theta_t})| \right] \\ &\leq \frac{1}{1-\gamma} \left[\sup_{\theta \in \Theta} L_{\text{PAE}}(\theta; \rho_\gamma^\pi) + \left\| \frac{d\rho_\gamma^\pi}{d\mu} \right\|_\infty (1 \vee W) \left(4\sqrt{\frac{Q_{\max}\beta}{T}} + \varepsilon_{\text{model}} \right) \right], \end{aligned}$$

which is the desired result. \square

The proof is the same as the proof of Corollary 6.14 of Agarwal et al. (2019) with the difference of the argument in (29), which relates the ε -stationarity w.r.t. the true dynamics to the same quantity w.r.t. the estimated dynamics.

We use this theorem along Theorem 2 on PG error estimate in order to provide the following convergence rate for the class of exponentially parameterized policies.

Theorem 5. Consider any distributions $\rho, \mu, \nu \in \bar{\mathcal{M}}(\mathcal{X})$. Let the policy π_θ be in the exponential family (16) with $\theta \in \Theta$ and Θ being a convex subset of \mathbb{R}^d . Assume that $\|\phi(a|x)\|_2 \leq B$ for any $(x, a) \in \mathcal{X} \times \mathcal{A}$. Suppose that the value function is bounded by Q_{\max} , the MDP has a finite number of actions $|\mathcal{A}|$, and $\frac{1}{2} \leq \gamma < 1$. Let $\beta = B^2 Q_{\max} \left[\frac{8\gamma|\mathcal{A}|^2}{(1-\gamma)^2} + \frac{6|\mathcal{A}|}{1-\gamma} \right]$. Let T be an integer number. Starting from a $\pi_{\theta_0} \in \Pi$, consider the sequence of policies $\pi_{\theta_1}, \dots, \pi_{\theta_T}$ generated by the projected model-based PG algorithm (25) with step-size $\eta = \frac{1}{\beta}$. Let $W = \sup_{\theta \in \Theta} \|w^*(\theta; \rho_\gamma^\pi)\|_2$, and assume that $W < \infty$. We then have

$$\begin{aligned} \min_{t=0,\dots,T} J_\rho(\bar{\pi}) - J_\rho(\pi_{\theta_t}) &\leq \\ \frac{1}{1-\gamma} &\left[\sup_{\theta \in \Theta} L_{\text{PAE}}(\theta; \rho_\gamma^\pi) + \frac{4BQ_{\max}}{1-\gamma} c_{\text{PG}}(\rho, \mu; \bar{\pi}) (1 \vee W) \left(4|\mathcal{A}| \sqrt{\frac{14\gamma}{T}} + \frac{\gamma}{1-\gamma} e_{\text{model}} \right) \right]. \end{aligned}$$

with

$$e_{\text{model}} = \begin{cases} \sup_{\theta \in \Theta} c_{\text{PG}}(\mu, \nu; \pi_\theta) \|\Delta \mathcal{P}^{\pi_\theta}\|_{1,1(\nu)}, \\ 2 \sup_{\theta \in \Theta} \|\Delta \mathcal{P}^{\pi_\theta}\|_{1,\infty}. \end{cases}$$

Proof. For the exponential family policy parameterization (16), Proposition 9 shows that Assumption A1 is satisfied with the choice of $\beta_1 = 2B$ and $\beta_2 = 6B^2$. We may now apply Theorem 4. To provide an upper bound for $\varepsilon_{\text{model}}$ in that theorem, we apply Theorem 2. After some simplifications applicable for $\gamma \geq 1/2$, we obtain the desired result. \square

Notice that the choice of $\gamma \geq 1/2$ is only to simplify the upper bound, and a similar result holds for any $\gamma \in [0, 1)$.

This theorem relates the performance of the best policy obtained as a result of T iterations of the PG algorithm to the number of iterations T , the distribution mismatch between $c_{\text{PG}}(\rho, \mu; \bar{\pi})$,

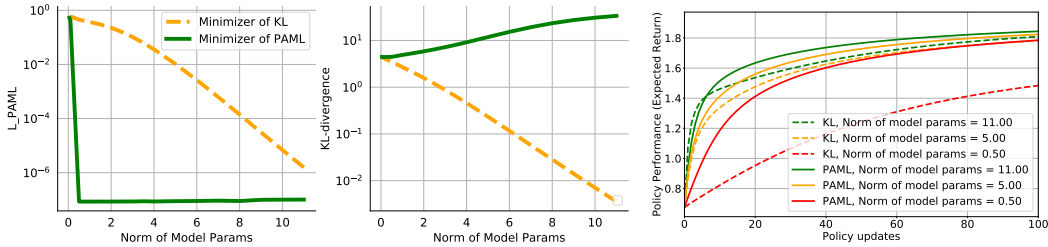


Figure 3: Results for finite 3-state MDP defined in Appendix C. (Top) Comparison of the minimizers of the PAML loss and the KL-divergence as a function of the maximum allowable norm of model parameters. The true model’s parameter norm would be close to 11.0 as measured by minimizing the KL without constraints. (Bottom) Policy performance as a function of model loss and (maximum allowed) norm of model parameters. Note that there is no estimation error in this setting.

some quantities related to the MDP and policy space, and in particular to the model error e_{model} . Combined with the results of the previous section, it shows that if the PG’s are estimated with enough accuracy, the policy obtained by an MBPG algorithm converges to the best policy in the class.

5 Empirical Studies

We compare the performance of PAML and MLE in a complete MBRL framework, as in Algorithm 1. We first present an illustrative example of PAML and MLE for a finite-state MDP. We then discuss how the loss introduced in Section 3 can be formulated for two PG-based planners, namely REINFORCE (Williams, 1992) and DDPG (Lillicrap et al., 2015). Details for reproducing these results can be found in the Appendix .

We illustrate the difference between PAML and MLE on a finite 3-state MDP and 2-state MDP . In this setting, we can calculate exact PGs with no estimation error, and thus the exact PAML loss, and KL-divergence. The details of the MDPs are provided in Appendix C. In these experiments, we use Projected Gradient Descent (PGD) to update the model parameters and constrain their L_2 norm, in order to limit model capacity. In Figures 3 and 4 (Top), we compare the PAML loss and KL-divergence of models trained to minimize each for a fixed policy. We see that the PAML loss of a model trained to minimize PAML is (as expected) much lower than that of a model trained to minimize KL. Note that the PAML loss of the KL minimizer decreases as the constraint on the model parameters is relaxed, whereas the minimizer of PAML is much less dependent on model capacity.

We also evaluate the performance of policies learned using these models, in a process similar to Algorithm 1, but with exact values rather than sampled ones. Figures 3 and 4 (Bottom), as the norm of the model parameters becomes smaller, the performance of the KL agent drops significantly compared to the PAML agent. However, when the constraint is relaxed (i.e. increased), the KL agent performs similarly to the PAML one. This example provides justification for the use of PAML: when the model space is constrained, such that it does not contain \mathcal{P}^* , PAML is able to learn a model that is more useful for planning.

For more thorough evaluation, we test PAML on three continuous control environments: Linear

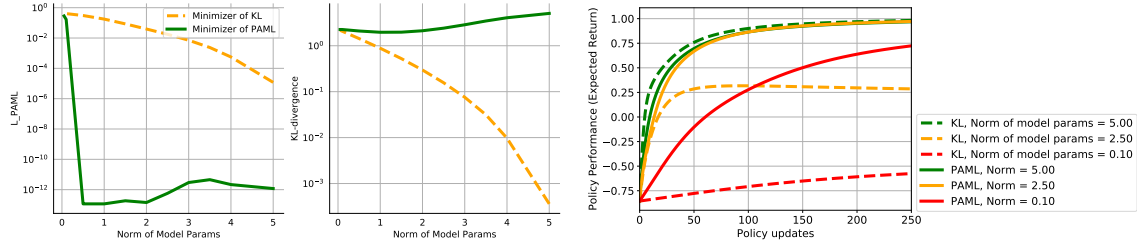


Figure 4: Results for finite 2-state MDP defined in Appendix C. (Top) Comparison of the minimizers of the PAML loss and the KL-divergence as a function of the maximum allowable norm of model parameters. The true model’s parameter norm would be close to 5.0 as measured by minimizing the KL without constraints. (Bottom) Policy performance as a function of model loss and norm of model parameters. Note that there is no estimation error in this setting.

Quadratic Regulation (LQR), Pendulum, and HalfCheetah. Pendulum and HalfCheetah are based on the OpenAI Gym framework (Brockman et al., 2016). The goal is to see if PAML performs better than MLE when the model class is constrained, or when the agent’s observations contain some extra dimensions irrelevant to the task. If the model class is not constrained, an MLE agent should perform well since it can represent the dynamics exactly. Otherwise, the transition dynamics cannot be represented exactly, and we expect PAML to perform better since it uses the available model capacity to find the best direction of improvement. We also evaluate the performance of the model-free method used (REINFORCE or DDPG) for reference.

To simulate the effect of having more dimensions in the observations than the underlying state, we concatenate to the state a vector of irrelevant or redundant information. For an environment that has underlying state x_t at time t , where $x_t \in \mathbb{R}^d$, the agent’s observation is given in one of the following ways :

1. **Random irrelevant dimensions:** $(x_t, \eta) \in \mathbb{R}^{d+n}$, where $\eta \sim \mathcal{N}_n(0, 1)$
2. **Correlated irrelevant dimensions:** $(x_t, \eta_t) \in \mathbb{R}^{d+n}$, where $\eta_t = \eta_0^t$ and $\eta_0 \sim \text{Unif}(0, 1)$. n can be chosen by the user. We show results for a few cases.
3. **Linear redundant dimensions:** $(x_t, W^T x_t) \in \mathbb{R}^{2d}$, where $W \sim \text{Unif}_{d \times d}(0, 1)$
4. **Non-linear redundant dimensions:** $(x_t, \cos(x_t), \sin(x_t)) \in \mathbb{R}^{3d}$
5. **Non-linear and linear redundant dimensions:** $(x_t, \cos(x_t), \sin(x_t), W^T x_t) \in \mathbb{R}^{4d}$, where $W \sim \text{Unif}_{d \times d}(0, 1)$

In this way, the agent’s observation vector is higher-dimensional than the underlying state, and it contains information that would not be useful for a model to learn. In the most general case, this may be replaced by the full-pixel observations, which contain more information than is necessary for solving the problem. To illustrate the differences between model learning methods, we choose to forgo evaluations over pixel inputs for the scope of this work. Although differentiating between useful state variables and irrelevant variables generated by concatenating noise may be overly simplistic (for example, a certain set of pixels could convey both useful and unnecessary information that the model may not know are unnecessary), it is an approximation that can nevertheless highlight the weakness of purely predictive model learning.

To train the model using MLE, we minimize the squared ℓ_2 distance between predicted and true next states for time-steps $1 \leq t \leq T$, where T is the length of each trajectory. The point-wise loss for time-step t and episode $1 \leq i \leq n$ would then be

$$c(X_{t:t+h}, \hat{X}_{t:t+h}; w) = \frac{1}{N} \sum_{i=1}^N \sum_{h=1}^H \left\| (\hat{X}_{t+h}^{(i)} - \hat{X}_{t+h-1}^{(i)}) - (X_{t+h}^{(i)} - X_{t+h-1}^{(i)}) \right\|_2^2, \quad (30)$$

where \hat{X} are the states predicted by the model, i.e. $\hat{X}_{t+1} \sim \hat{\mathcal{P}}^\pi(\cdot | X_t, A_t)$ and similarly X are the states given by the true environment, \mathcal{P}^* .

This is a multi-step prediction loss with horizon H . This loss is the empirical negative-log likelihood, assuming that $\mathcal{P}^*(\cdot | x)$ is Gaussian with fixed variance. Our model in all experiments is deterministic and directly predicts $\Delta \hat{X} = \hat{X}_{t+h}^{(i)} - \hat{X}_{t+h-1}^{(i)}$. Moreover, for the REINFORCE experiments, we set H to be the length of the trajectory, and for the DDPG ones we set it to 1.

Since PAML is planner-aware, the formulation of the loss changes depending on the planner used. To form the PAML loss compatible with REINFORCE as the planner, the model gradient is obtained according to case (10b). Namely, the model returns are calculated by unrolling $\hat{\mathcal{P}}^\pi$ (and the true returns from data collected for every episode). The PG for the model is calculated on states from the real environment, which, since REINFORCE calculates full-episode returns, come only from the first states of each episode. Thus, the model and true PG's are calculated over the starting state distribution ρ , whereas the returns are calculated over $\hat{\mathcal{P}}^\pi$ and $\mathcal{P}^{*\pi}$ respectively. In practice, we find that calculating the ℓ_2 distance between the true PG and model PG separately for each starting state gives better results than first averaging the PGs over all starting states and then calculating the ℓ_2 distances. During planning, we use the mean returns as a baseline for reducing the variance of the REINFORCE gradients. We evaluate this formulation of the algorithm on a simple LQR problem, the details of which can be found in Appendix C. The extra dimensions used for these experiments were random noise, defined as type 1 above.

The results for this formulation are shown in Figure 6 for the LQR problem with trajectories of 200 steps. The performance of agents trained with PAML, MLE, and REINFORCE (model-free) are shown over 200,000 steps. It can be seen that both model-based methods learn more slowly as irrelevant dimensions are added (the model-free method learns slowly for all cases). For no irrelevant dimensions, MLE learns faster than PAML. This is expected as in this case, an MLE model should be able to recover the underlying dynamics easily, making it a good model-learning strategy. However, as the number of irrelevant dimensions are increased, PAML shows better performance than MLE. This is encouraging as it shows that PAML is not as affected by irrelevant information.

It is also possible to use PAML with an actor-critic planner. We use the DDPG algorithm as the planner which uses a deterministic policy and explores using correlated noise (Lillicrap et al., 2015), and leave other actor-critic experiments to future work. Our PAML formulation corresponds to case (10a): the model PG is calculated using the future-state distribution of $\hat{\mathcal{P}}^\pi$, and the true PG using samples from $\mathcal{P}^{*\pi}$. The action-value function (critic) for both the model PG and true PG is learned using $\mathcal{P}^{*\pi}$ samples.

Since the PAML loss depends on the critic (see (8)), we train the critic for extra steps without changing the policy. After every iteration of data collection from the environment, the critic is trained on true data by minimizing the mean-squared temporal difference (TD) error,

$$L(Q; Q') = \frac{1}{N} \sum_i (R_i + \gamma Q'(X_{i+1}, \pi'(X_{i+1})) - Q(X_i, \pi(X_i)))^2,$$

where Q', π' are the target critic and actor, updated using soft updates as shown in (Lillicrap et al., 2015). In contrast to the REINFORCE formulation, we calculate the ℓ_2 -distance between the model PG and true PG averaged over all states, rather than separately for each starting state. To control for the effect of a critic that has been trained for multiple steps, we perform the critic pre-training for the model-free and MLE experiments as well. In addition, for this formulation, we present experiments for no extra dimensions added to the observations, and also for extra dimensions of types 2, 3, 4 and 5 added.

The results are shown in Figures 7 and 8. For these experiments, we use a model size that is smaller than what is typically used for MB solutions of this environment (e.g. see Kurutach et al. (2018), Chua et al. (2018), Nagabandi et al. (2018)). This model size is chosen in order to constrain the model class. In addition, the planning horizon is longer than typical (see the supplementary materials for comparison of planning horizon performances). Note the poor performance of MLE in HalfCheetah even in the presence of no irrelevant dimensions. We observe that PAML generally performs better than MLE, especially when redundant extra dimensions are present. Although both models perform worse as irrelevant dimensions are added, PAML’s performance does not degrade as much as MLE and is able to outperform MLE in this constrained model class. This is most notable in the case of the high(17)-dimensional HalfCheetah environment. This may be because MLE with limited model capacity is not able to learn to predict accurately as the complexity of the environment increases. In contrast, in the 3-dimensional Pendulum-v0 environment, the MLE can predict next states well enough not to degrade policy performance even when model capacity is low and there are irrelevant or redundant observations.

5.1 Effect of model size and planning horizon on HalfCheetah model-based performance

The performance of the model-based experiments on the HalfCheetah environment mirrored their performance on the finite-state MDPs. As can be seen in Figure 5, PAML performs better than MLE when the model size is constrained to be less than what is known to be ideal for this environment (512 neurons, see for example Kurutach et al. (2018), Chua et al. (2018), Nagabandi et al. (2018)). We also show results for the higher capacity model, demonstrating that MLE indeed performs better when the model capacity is not constrained. In addition, we see that as the planning horizon is lowered, and the planning portion of the problem becomes less of a bottleneck, PAML and MLE performance become very close. Note that in all experiments, the critic undergoes pre-training, leading to improved performance in the model-free case as well.

6 Discussion and Future Work

We introduced Policy-Aware Model Learning, a decision-aware MBRL framework that incorporates the policy in the way the model is learned. PAML encourages the model to learn about aspects of the environment that are relevant to planning by a PG method, instead of trying to build an accurate predictive model. We provided a generic PG error guarantee based on the error between the models. Furthermore, we proved a convergence guarantee for a generic model-based PG algorithm. We empirically evaluated PAML and compared it with MLE on a number of benchmark domains.

The current loss formulation of PAML relies on having an estimate of critic. Studying the effect of error in critic on PAML or perhaps even defining a loss function that is critic-independent, if

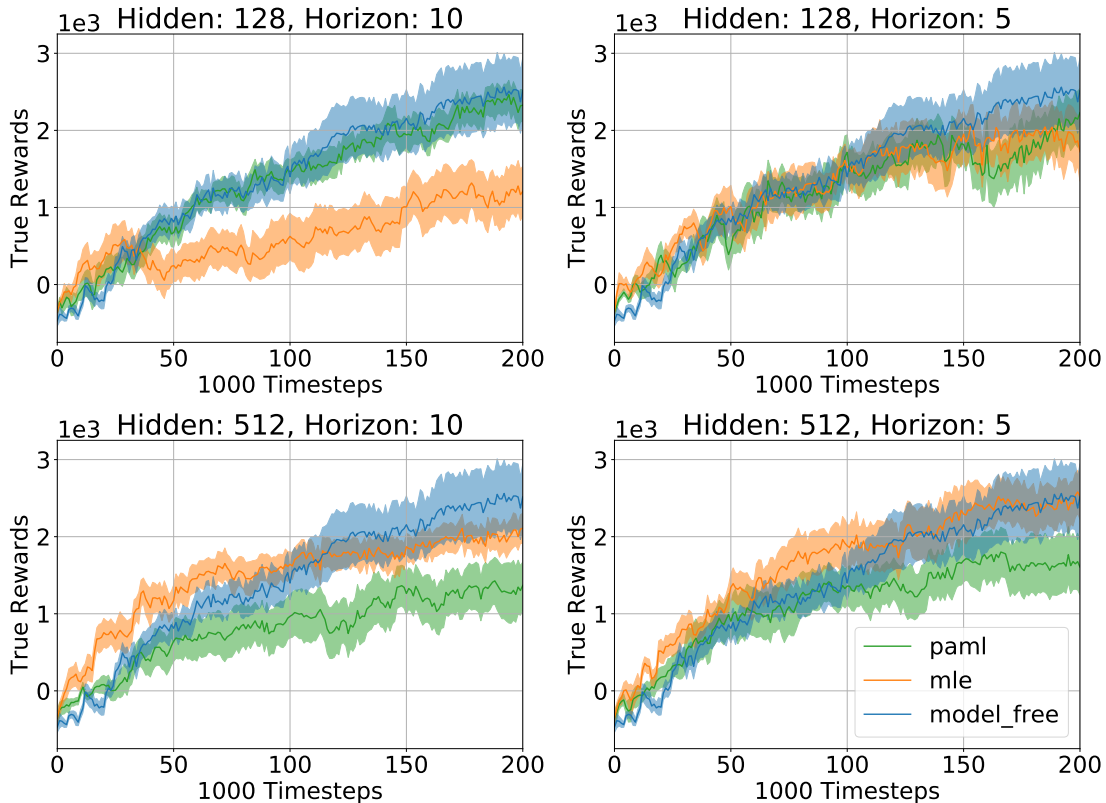


Figure 5: Performance of policies trained using model-based and model-free versions of DDPG on HalfCheetah. For the model-based agents, the hidden-size and planning horizons are displayed in the titles. The model used for all model-based experiments is a 2-layer neural network with ReLU activations on the hidden layer (and hidden size as written). The solid lines indicate the mean of 10 runs and the shaded regions depict the standard error.

possible, are interesting future research directions. Another fruitful direction is deriving PAML loss for other PG methods.

A Theoretical Background and Proofs

A.1 Background Results

We report some background results in this section. These results are quoted from elsewhere, with possibly minor modification, as shall be discussed.

Lemma 6 (Lemma E.5 of Agarwal et al. 2019). *Suppose that Assumption A1 holds, the action space is finite with $|\mathcal{A}|$ elements, and the action-value functions are all $Q_{max} = \frac{R_{max}}{1-\gamma}$ -bounded. For*

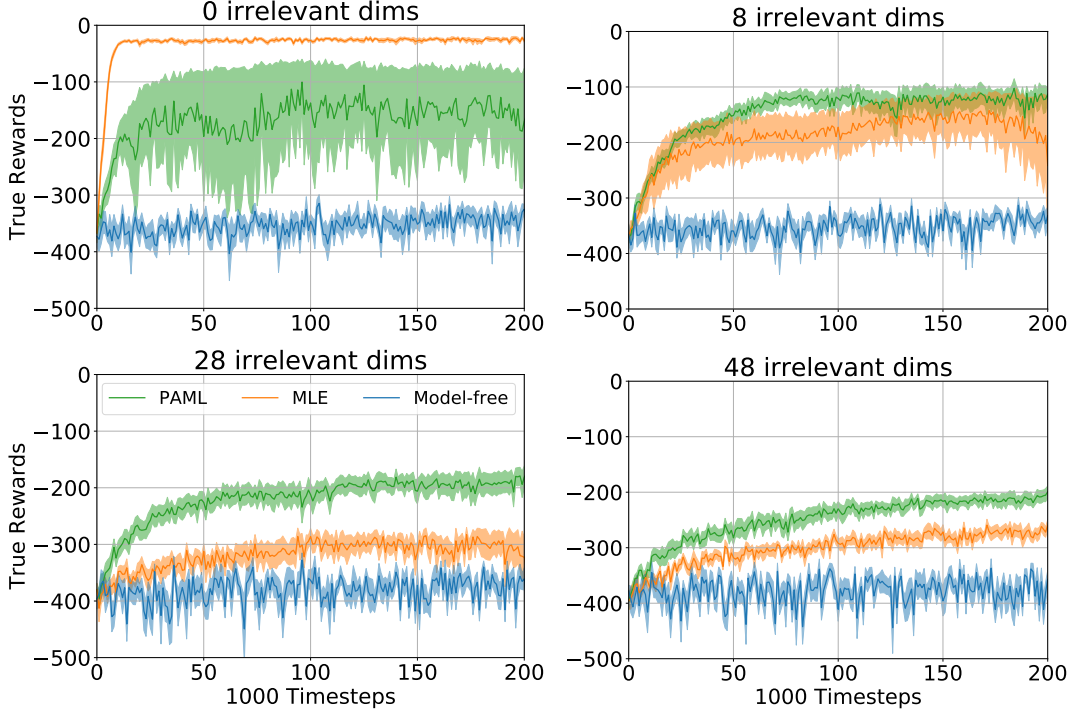


Figure 6: Performance of policies trained model-based with REINFORCE as the planner for different numbers of irrelevant dimensions added to the state observations. The solid lines indicate the mean of 10 runs and the shaded regions depict the standard error.

any $x \in \mathcal{X}$, we then have

$$\|\nabla_{\theta} V^{\pi_{\theta_1}}(x) - \nabla_{\theta} V^{\pi_{\theta_2}}(x)\|_2 \leq \beta \|\theta_1 - \theta_2\|_2,$$

with

$$\beta = Q_{\max} \left[\frac{2\gamma\beta_1^2|\mathcal{A}|^2}{(1-\gamma)^2} + \frac{\beta_2|\mathcal{A}|}{1-\gamma} \right].$$

The difference of this result with the original Lemma E.5 of Agarwal et al. (2019) is that here we assume that the rewards are R_{\max} -bounded, whereas their paper is based on the assumption that the reward is between 0 and 1. As such, their Q_{\max} is $\frac{1}{1-\gamma}$, and their β is $\frac{2\gamma\beta_1^2|\mathcal{A}|^2}{(1-\gamma)^3} + \frac{\beta_2|\mathcal{A}|}{(1-\gamma)^2}$.

The change in the proof of Lemma E.5 stems from the change in Lemma E.2 of Agarwal et al. (2019). The upper bound in Lemma E.2 changes from

$$\max_{\|u\|_2=1, \theta+\alpha u \in \Theta} \left| \frac{d^2 \tilde{V}(\alpha)}{d\alpha^2} \Big|_{\alpha=0} \right| \leq \frac{2\gamma C_1^2}{(1-\gamma)^3} + \frac{C_2}{(1-\gamma)^2}$$

to $Q_{\max} \left[\frac{2\gamma C_1^2}{(1-\gamma)^2} + \frac{C_2}{1-\gamma} \right]$.

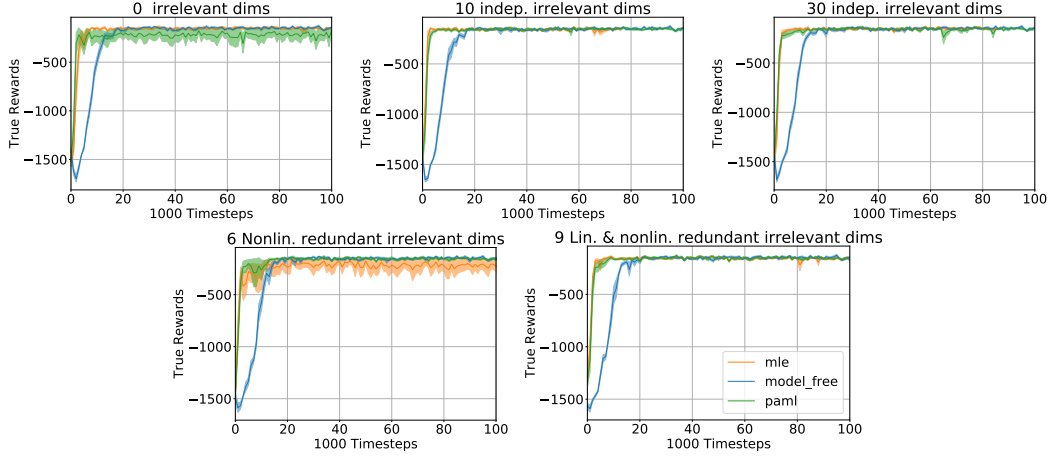


Figure 7: Performance of policies for different numbers of irrelevant and redundant dimensions added to the state observations for the locomotion problem Pendulum-v0, the details of which can be found in the Appendix

Proposition 7 (Proposition D.1 of Agarwal et al. (2019)). Let $\hat{J}_\mu(\pi_\theta)$ be β -smooth in θ . Define the gradient mapping as

$$G^\eta(\theta) = \frac{1}{\eta} \left(\text{Proj}_\Theta \left[\theta + \eta \nabla_\theta \hat{J}_\mu \right] - \theta \right).$$

Let $\theta' = \theta + \eta G^\eta$ for some $\eta > 0$. We have

$$\max_{\theta + \delta \in \Theta, \|\delta\|_2 \leq 1} \delta^\top \nabla_\theta \hat{J}_\mu(\pi_{\theta'}) \leq (\eta\beta + 1) \|G^\eta(\theta)\|_2.$$

The following lemma is a multivariate form of the mean value theorem. It is not a new result, but for the sake of completeness, we report it here.² This statement and proof is quoted from the extended version of Huang et al. (2015).

Lemma 8. Let $f : \mathbb{R}^m \rightarrow \mathbb{R}^m$ be a continuously differentiable function and $J : \mathbb{R}^m \rightarrow \mathbb{R}^{m \times m}$ be its Jacobian matrix, that is $J_{ij} = \frac{\partial f_i(x)}{\partial x_j}$. We then have for any $x, \Delta x \in \mathbb{R}^m$,

$$\|f(x + \Delta x) - f(x)\|_2 \leq \sup_{x'} \|J(x')\|_2 \|\Delta x\|_2,$$

$$\|f(x + \Delta x) - f(x)\|_1 \leq \sup_{x'} \|J(x')\|_1 \|\Delta x\|_1.$$

An l_1 and l_2 matrix norms in this lemma are vector-induced norms on \mathbb{R}^m , and have the property that for an $m \times m$ matrix A , $\|A\|_2 = \sigma_{\max}(A)$ and $\|A\|_1 = \max_j \sum_i |A_{ij}|$.

Proof. Consider a continuously differentiable function $g : \mathbb{R} \rightarrow \mathbb{R}$. By the fundamental theorem of calculus, $g(1) - g(0) = \int_0^1 g'(t) dt$. For each component f_i of f , define $g_i(u) = f_i(x + u\Delta x)$,

²One can find its proof on Wikipedia page on the [Mean value theorem](#).

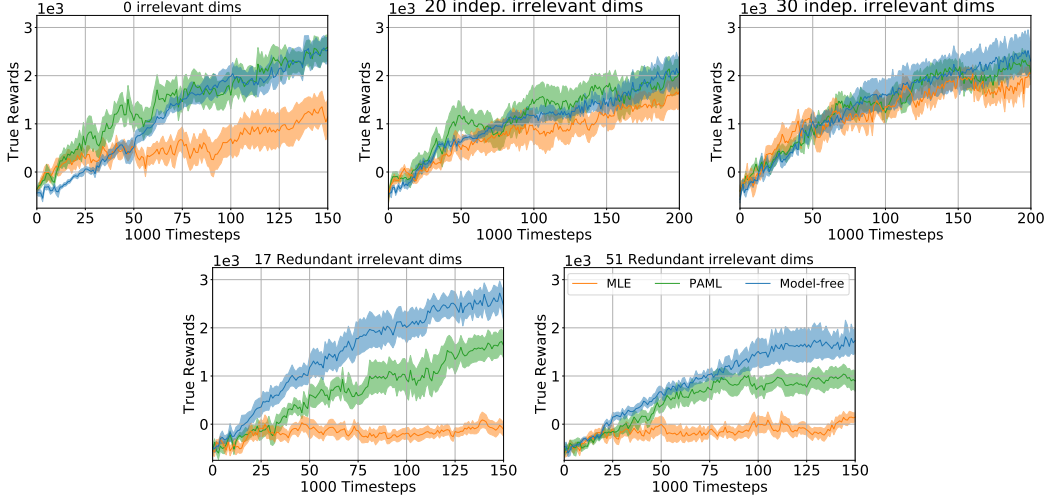


Figure 8: Performance of policies for different numbers of irrelevant and redundant dimensions added to the state observations for the locomotion problem HalfCheetah-v2, the details of which can be found in the Appendix.

so $f_i(x + \Delta x) - f_i(x) = g_i(1) - g_i(0) = \int_0^1 g'_i(t) dt = \int_0^1 \left[\sum_{j=1}^d \frac{\partial f_i}{\partial x_j}(x + t\Delta x) \Delta x_j \right] dt$. For the vector-valued function f , we get $f(x + \Delta x) - f(x) = \int_0^1 J(x + t\Delta x) \Delta x dt$, therefore,

$$\begin{aligned} \|f(x + \Delta x) - f(x)\|_2 &= \left\| \int_0^1 J(x + t\Delta x) \Delta x dt \right\|_2 \leq \int_0^1 \|J(x + t\Delta x)\|_2 \|\Delta x\|_2 dt \\ &\leq \sup_{x'} \|J(x')\|_2 \|\Delta x\|_2 \int_0^1 dt. \end{aligned}$$

The l_1 -norm result is obtained using the l_1 -norm instead of the l_2 -norm in the last step. \square

A.2 Auxiliary Results

Proposition 9. Consider a policy π_θ with the policy parameterization (16). Assume that $\|\phi(a|x)\|_2 \leq B$ for any $(x, a) \in \mathcal{X} \times \mathcal{A}$. This policy satisfies Assumption A1 (Section 4.2) with

$$\beta_1 = 2B, \quad \beta_2 = 6B^2.$$

Proof. We use Taylor series expansion of π_θ and the mean value theorem in order to find the Lipschitz and smoothness constants. We start by computing the gradient and the Hessian of the policy. We can fix $(x, a) \in \mathcal{X} \times \mathcal{A}$ in the rest. For the policy $\pi_\theta = \pi_\theta(a|x) = \frac{\exp(\phi^\top(a|x)\theta)}{\int \exp(\phi^\top(a'|x)\theta) da'}$, the gradient is

$$\begin{aligned} \frac{\partial \pi_\theta}{\partial \theta} &= \pi_\theta(a|x) (\phi(a|x) - \mathbb{E}_{\pi_\theta(\cdot|x)} [\phi(A|x)]) \\ &= \pi_\theta(a|x) (\phi(a|x) - \bar{\phi}_\theta) = \pi_\theta(a|x) \Delta \phi_\theta, \end{aligned} \tag{31}$$

where we use $\bar{\phi}_\theta = \bar{\phi}_\theta(x) = \mathbb{E}_{\pi_\theta(\cdot|x)}[\phi(A|x)]$ and $\Delta\phi_\theta = \phi(a|x) - \bar{\phi}_\theta$ as more compact notations. Likewise, the Hessian H_θ of π_θ is

$$H_\theta = \frac{\partial^2 \pi_\theta(a|x)}{\partial \theta^2} = \frac{\partial \pi_\theta}{\partial \theta} \Delta\phi_\theta^\top + \pi_\theta \frac{\partial \Delta\phi_\theta^\top}{\partial \theta} = \pi_\theta \left[\Delta\phi_\theta \Delta\phi_\theta^\top + \frac{\partial \Delta\phi_\theta^\top}{\partial \theta} \right].$$

We compute $\frac{\partial \Delta\phi_\theta^\top}{\partial \theta}$ as follows:

$$\begin{aligned} \frac{\partial \Delta\phi_\theta^\top}{\partial \theta} &= -\frac{\partial \mathbb{E}_{\pi_\theta(\cdot|x)}[\phi(A|x)^\top]}{\partial \theta} = -\int \frac{\partial \pi_\theta}{\partial \theta} \phi(a)^\top da = -\int \pi_\theta(a|x) (\phi(a|x) - \bar{\phi}_\theta) \phi(a)^\top da \\ &= \bar{\phi}_\theta(x) \bar{\phi}_\theta^\top(x) - \mathbb{E}[\phi(A|x)\phi(A|x)^\top] = -\mathbf{Cov}_{\pi_\theta(\cdot|x)}(\phi(A|x)). \end{aligned}$$

Therefore,

$$\begin{aligned} H_\theta &= \pi_\theta \left[\Delta\phi_\theta \Delta\phi_\theta^\top + \bar{\phi}_\theta \bar{\phi}_\theta^\top - \mathbb{E}_{\pi_\theta}[\phi(A|x)\phi(A|x)^\top] \right] \\ &= \pi_\theta \left[\Delta\phi_\theta \Delta\phi_\theta^\top - \mathbf{Cov}_{\pi_\theta(\cdot|x)}(\phi(A|x)) \right]. \end{aligned} \quad (32)$$

Consider two points $\theta_1, \theta_2 \in \Theta$. By the mean value theorem, there exists a θ' on the line segment connecting θ_1 and θ_2 (that is, $\theta' = (1-t)\theta_1 + t\theta_2$ with $t \in (0, 1)$) such that $\pi_{\theta_2}(a|x) - \pi_{\theta_1}(a|x) = \nabla_\theta \pi_{\theta'}(a|x) \Big|_{\theta_1 \leq \theta' \leq \theta_2} (\theta_2 - \theta_1)$. Therefore,

$$|\pi_{\theta_2}(a|x) - \pi_{\theta_1}(a|x)| \leq \sup_{\theta'} \|\nabla_\theta \pi_{\theta'}(a|x)\|_2 \|\theta_2 - \theta_1\|_2.$$

By (31), we have that for any θ' ,

$$\|\nabla_\theta \pi_{\theta'}(a|x)\|_2 \leq \pi_{\theta'}(a|x) \|\phi(a|x) - \bar{\phi}_{\theta'}(x)\|_2 \leq \pi_{\theta'}(a|x) (\|\phi(a|x)\|_2 + \mathbb{E}[\|\phi_{\theta'}(A|x)\|_2]) \leq 2B.$$

This shows that

$$|\pi_{\theta_2}(a|x) - \pi_{\theta_1}(a|x)| \leq 2B \|\theta_2 - \theta_1\|_2.$$

Lemma 8 in Appendix A.2, which can be thought of as the vector-valued version of the mean value theorem (though it is only an inequality), shows that for any θ_1, θ_2 , we have

$$\|\nabla_\theta \pi_{\theta_1}(a|x) - \nabla_\theta \pi_{\theta_2}(a|x)\|_2 \leq \sup_{\theta'} \|H_{\theta'}\|_2 \|\theta_1 - \theta_2\|_2,$$

where $\|H_{\theta'}\|_2$ is the ℓ_2 -induced matrix norm. From (32), we have that for any θ , including θ' ,

$$\begin{aligned} \|H_\theta\|_2 &\leq \pi_\theta \left[\|\Delta\phi_\theta \Delta\phi_\theta^\top\|_2 + \|\bar{\phi}_\theta \bar{\phi}_\theta^\top\|_2 + \|\mathbb{E}_{\pi_\theta}[\phi(A|x)\phi(A|x)^\top]\|_2 \right] \\ &\leq \pi_\theta(a|x) \left[\|\Delta\phi_\theta\|_2^2 + \|\bar{\phi}_\theta\|_2^2 + \mathbb{E}_{\pi_\theta}[\|\phi(A|x)\|_2^2] \right] \leq 6B^2, \end{aligned}$$

where we used the fact that for a vector $u \in \mathbb{R}^d$, the ℓ_2 -induced matrix norm of uu^\top is $\|u\|_2^2$, in addition to the the convexity of norm along with the Jensen inequality. This shows that

$$\|\nabla_\theta \pi_{\theta_1}(a|x) - \nabla_\theta \pi_{\theta_2}(a|x)\|_2 \leq 6B^2 \|\theta_2 - \theta_1\|_2.$$

□

B Further Detail on VAML and Comparison with PAML

This section provides more detail on Value-Aware Model Learning (VAML) and Iterative VAML (IterVAML) (Farahmand et al., 2016a, 2017; Farahmand, 2018), and complements the discussion in Section 2. For more detail and the results on the properties of VAML and IterVAML, refer to the original papers.

Recall that VAML attempts to find $\hat{\mathcal{P}}$ such that applying the Bellman operator $T_{\hat{\mathcal{P}}}^*$ according to the model $\hat{\mathcal{P}}$ on a value function Q has a similar effect as applying the true Bellman operator $T_{\mathcal{P}^*}^*$ on the same function, i.e.,

$$T_{\hat{\mathcal{P}}}^*Q \approx T_{\mathcal{P}^*}^*Q.$$

This ensures that one can replace the true dynamics with the model without (much) affecting the internal mechanism of a Bellman operator-based Planner. This goal can be realized by defining the loss function as follows: Assuming that V (or Q) is known, the pointwise loss between $\hat{\mathcal{P}}$ and \mathcal{P}^* is

$$c(\hat{\mathcal{P}}, \mathcal{P}^*; V)(x, a) = \left| \left\langle \mathcal{P}^*(\cdot|x, a) - \hat{\mathcal{P}}(\cdot|x, a), V \right\rangle \right| = \left| \int \left[\mathcal{P}^*(dx'|x, a) - \hat{\mathcal{P}}(dx'|x, a) \right] V(x') \right|, \quad (33)$$

in which we substituted $\max_a Q(\cdot, a)$ in the definition of the Bellman optimality operator (2) with V to simplify the presentation.

By taking the expectation over state-action space according to the probability distribution $\nu \in \mathcal{M}(\mathcal{X} \times \mathcal{A})$, which can be the same distribution as the data generating one, VAML defines the expected loss function

$$c_{2,\nu}^2(\hat{\mathcal{P}}, \mathcal{P}^*; V) = \int d\nu(x, a) \left| \int \left[\mathcal{P}^*(dx'|x, a) - \hat{\mathcal{P}}(dx'|x, a) \right] V(x') \right|^2. \quad (34)$$

As the value function V is unknown, we cannot readily minimize this loss function, or its empirical version. Handling this unknown V differentiates the original formulation introduced by Farahmand et al. (2017) with the iterative one (Farahmand, 2018). Briefly speaking, the original formulation of VAML considers that Planner represents the value function within a known function space \mathcal{F} , and it then tries to find a model that no matter what value function $V \in \mathcal{F}$ is selected by the planner, the loss function (34) is still small. This leads to a robust formulation of the loss in the form of

$$c_{2,\nu}^2(\hat{\mathcal{P}}, \mathcal{P}^*) = \int d\nu(x, a) \sup_{V \in \mathcal{F}} \left| \int \left[\mathcal{P}^*(dx'|x, a) - \hat{\mathcal{P}}(dx'|x, a) \right] V(x') \right|^2. \quad (35)$$

Even though taking the supremum over \mathcal{F} makes this loss function conservative compared to (34), where the value function V is assumed to be known, it is still a tighter objective to minimize than the KL divergence. Consider a fixed $z = (x, a)$, and notice that we have

$$\sup_{V \in \mathcal{F}} |\langle \mathcal{P}^*(\cdot|x, a) - \hat{\mathcal{P}}(\cdot|x, a), V \rangle| \leq \left\| \mathcal{P}_z^* - \hat{\mathcal{P}}_z \right\|_1 \sup_{V \in \mathcal{F}} \|V\|_\infty \leq \sqrt{2\text{KL}(\mathcal{P}_z^* \|\hat{\mathcal{P}}_z)} \sup_{V \in \mathcal{F}} \|V\|_\infty, \quad (36)$$

where we used Pinsker's inequality in the second inequality. MLE is the minimizer of the KL-divergence based on the empirical distribution (i.e., data), so these upper bounds suggest that if we find a good MLE (with a small KL-divergence), we also have a model that has a small total

variation error too. This in turn implies the accuracy of the Bellman operator according to the learned model.

Nonetheless, these sequences of upper bounding might be quite loose. As an extreme, but instructive, example, consider that the value function space consisting of bounded constant functions ($\mathcal{F} = \{x \mapsto c : |c| < \infty\}$). For this function space, $\sup_{V \in \mathcal{F}} |\langle \mathcal{P}^*(\cdot|x, a) - \hat{\mathcal{P}}(\cdot|x, a), V \rangle|$ is always zero, irrespective of the the total variation and the KL-divergence of two distributions. MLE does not explicitly benefit from these interaction of the value function and the model. For more detail and discussion, refer to [Farahmand et al. \(2017\)](#).

The Iterative VAML (IterVAML) formulation of [Farahmand \(2018\)](#) exploits some extra knowledge about how Planner works. Instead of only assuming that Planner uses the Bellman optimality operator without assuming any extra knowledge about its inner working (as the original formulation does), IterVAML considers that Planner is in fact an (Approximate) Value Iteration algorithm. Recall that (the exact) value iteration (VI) is an iterative procedure that performs

$$Q_{k+1} \leftarrow T_{\mathcal{P}^*}^* Q_k \triangleq r + \gamma \mathcal{P}^* V_k, \quad k = 0, 1, \dots$$

IterVAML benefits from the fact that if we have a model $\hat{\mathcal{P}}$ such that

$$\hat{\mathcal{P}} V_k \approx \mathcal{P}^* V_k,$$

the true dynamics \mathcal{P}^* can be replaced by the learned dynamics $\hat{\mathcal{P}}$ without much affecting the working of VI. IterVAML learns a new model at each iteration, based on data sampled from \mathcal{P}^* and the current approximation of the value function V_k . The learned model can then be used to perform one iteration of (A)VI.

It might be instructive to briefly compare the objective of VAML and PAML. VAML tries to minimize the error between the Bellman operator w.r.t. the model $\hat{\mathcal{P}}$ and the Bellman operator w.r.t. the true transition model \mathcal{P}^* . PAML, on the other hand, focuses on minimizing the error between the PG computed according to the model vs. the true transition model. Furthermore, (36), Theorem 2, and (20) show that the TV distance and the KL divergence provide an upper bound on the loss function of both VAML and PAML.

We may come up with a helpful perspective about these objectives by interpreting them as integral probability metrics (IPM) ([Müller, 1997](#)). Recall that given two probability distributions $\mu_1, \mu_2 \in \mathcal{M}(\mathcal{X})$ defined over the set \mathcal{X} and a space of functions $\mathcal{G} : \mathcal{X} \rightarrow \mathbb{R}$, the IPM distance is defined as

$$d_{\mathcal{G}}(\mu_1, \mu_2) = \sup_{g \in \mathcal{G}} \left| \int g(x) (\mathrm{d}\mu_1(x) - \mathrm{d}\mu_2(x)) \right|.$$

This distance is the maximal difference in expectation of a function g according to μ_1 and μ_2 when the test function g is allowed to be any function in \mathcal{G} . The TV distance is an IPM with \mathcal{G} being the set of bounded measurable function, cf. (12). This set is quite large. The original formulation of VAML limits the test functions to the space of value functions \mathcal{F} , see (36). If we choose \mathcal{G} to be the space of 1-Lipschitz functions, we obtain 1-Wasserstein distance. Therefore, if the space of value functions \mathcal{F} is the space of Lipschitz functions, VAML minimizes the Wasserstein distance between the true dynamics and the model, as observed by [Asadi et al. \(2018\)](#). But the space of value functions often has more structure and regularities than being Lipschitz (e.g., its functions have some kind of higher-order smoothness properties), in which case VAML's loss becomes smaller than Wasserstein distance. IterVAML further constrains the space of test function by choosing a particular test

function V_k at each iteration, that is $\mathcal{G} = \{V_k\}$. The test function for PAML is a single function too, different from IterVAML’s, and is defined as $g(x) = \mathbb{E}_{A \sim \pi_\theta(\cdot|x)} [\nabla_\theta \log \pi_\theta(A|x) Q^{\pi_\theta}(x, A)]$. The compared distributions, however, are not \mathcal{P}^* and $\hat{\mathcal{P}}$, but their discounted future-state distribution $\rho_\gamma(\cdot; \mathcal{P}^{*\pi_\theta})$ and $\rho_\gamma(\cdot; \hat{\mathcal{P}}^{\pi_\theta})$, cf. (11).

C Experimental Details

C.1 Environments

1. **Finite 2-state MDP.** We will use the following convention for this and the 3-state MDP defined next:

$$\begin{aligned} r(x_i, a_j) &= \mathbf{r}[i \times |\mathcal{A}| + j] \\ P(x_k|x_i, a_j) &= \mathbf{P}[i \times |\mathcal{A}| + j][k], \end{aligned}$$

where \mathbf{P}, \mathbf{r} are given below.

$$\begin{aligned} |\mathcal{A}| &= 2, |\mathcal{X}| = 2, \gamma = 0.9 \\ \mathbf{P} &= [[0.7, 0.3], [0.2, 0.8], [0.99, 0.01], [0.99, 0.01]] \\ \mathbf{r} &= [-0.45, -0.1, 0.5, 0.5] \end{aligned}$$

2. **Finite 3-state MDP.** Following the convention above:

$$|\mathcal{A}| = 2, |\mathcal{X}| = 3, \gamma = 0.9$$

$$\begin{aligned} \mathbf{P} &= [[[0.6, 0.399999, 0.000001], [0.1, 0.8, 0.1], [0.899999, 0.000001, 0.1]], \\ & \quad [[0.98, 0.01, 0.01], [0.2, 0.000001, 0.799999], [0.000001, 0.3, 0.699999]]] \\ \mathbf{r} &= [[0.1, -0.15], [0.1, 0.8], [-0.2, -0.1]] \end{aligned}$$

3. **LQR** is defined as follows:

$$x' = Ax + Bu; \quad r(x, u) = x^T x + u^T u; \quad u \sim \pi(a|x), \quad (37)$$

where $x, u \in \mathbb{R}^2$ and A is designed so that the system would be stable over time (i.e. if $u = 0, x \rightarrow 0$). Specifically,

$$A = \begin{bmatrix} 0.9 & 0.4 \\ -0.4 & 0.9 \end{bmatrix}.$$

The trajectory length is 201 steps (200 actions taken).

4. **Pendulum-v0** (OpenAI Gym) state dimensions: 3, action dimensions: 1, trajectory length: 201
5. **HalfCheetah-v2** (OpenAI Gym) state dimensions: 17, action dimensions: 6, trajectory length: 1001

C.2 Engineering details

For the finite-state MDP experiments, the policy is parameterized by $|\mathcal{X}| \times |\mathcal{A}|$ parameters with Softmax applied row-wise (over actions for each state). The model is parameterized by $|\mathcal{A}| \times |\mathcal{X}| \times |\mathcal{X}|$ parameters with Softmax applied to the last dimension (over states for each state, action pair). Calculation of policy gradients is done by solving for the exact value function and taking gradients with respect to the policy parameters using backpropagation. Hyperparameters for performance plots are as follows, model learning rate : 0.001, policy learning rate: 0.1, training iterations for model (per outer loop iteration): 200, training iterations for policy (per outer loop iteration): 1.

For the REINFORCE experiments, the policy is a 2-layer neural network (NN) with hidden size 64 and Rectified Linear Unit (ReLU) activations for the hidden layer. The second layer is separated for predicting the mean and log standard deviation (std) of a Gaussian policy (i.e. the first layer is shared for the mean and std but the second layer has separate weights for each). The output layer activations are Tanh for the mean and Softplus for the log std. The policy is trained with the Adam optimizer (Kingma & Ba, 2014) with learning rate 0.0001.

For the actor-critic formulation, the critic network is a 2-layer NN with hidden size 64 and ReLU activations for the hidden layer. The output layer has no nonlinearities. The policy is a 2-layer NN with hidden size 30 and ReLU activations for the hidden layer. The output layer has Tanh activations. Both the policy and actor are trained with the Adam optimizer with learning rates 0.0001 and 0.001, respectively. The soft update parameter (Lillicrap et al., 2015) for the target networks is 0.001.

The model architectures are as follows:

- LQR: Linear connection from input to output with no nonlinearities.
- Pendulum: two linear layers with hidden size 2. This is a linear model with a bottleneck as the states of the Pendulum environment are represented with 3 dimensions.
- HalfCheetah: 2-layer NN with hidden size 128, and ReLU activations on the hidden layer. The output layer has no nonlinearities.

The models in all experiments are optimized using stochastic gradient descent with no momentum and initial learning rates given in Table 1. The learning rates are reduced by an order of magnitude according to a schedule also given in Table 1. For each iteration of Alg. 1, the model is used to generate virtual samples for planning. Recalling that the model requires a starting state and action in order to predict the next state, the starting states used in our experiments are as follows: a fraction come directly from the replay buffer, of the rest, half are sampled from the starting state distribution of the environment (i.e. ρ), and half are uniformly randomly sampled from a neighbourhood of states from the replay buffer. For additional implementation details refer to the code.

	LQR (REINFORCE)	Pendulum-v0(DDPG)	HalfCheetah-v0(DDPG)
Initial model learning rate	MLE: 1e-5, PAML: 1e-4	MLE: 1e-4, PAML: 1e-3	MLE: 1e-5, PAML: 1e-3
LR schedule	[500,1200,1800] (training steps)	MLE: [10,1000,20000000], PAML: [10,500,1000] (iterations of Alg. 1)	
Number of transitions from real environment per iteration of Alg. 1	MLE: 1000, PAML: 1000	MLE: 1000, PAML: 1000	MLE: 200, PAML: 200
Number of virtual samples per iteration of Alg. 1	MLE: 2000 (episodes), PAML: 2000 episodes for irrelevant dimensions, 500 episodes for no irrelevant dimensions	MLE: 500, PAML: 500	MLE: 20, PAML: 20
Planning horizon	MLE: 200, PAML: 200	MLE: 10, PAML: 10	MLE: 10, PAML: 10
Fraction of planning data coming from replay buffer	MLE: 1.0, PAML: 1.0	MLE: 0.25, PAML: 0.25	MLE: 0.5, PAML: 0.5

Table 1: Experimental details for the results shown in this work.

References

- Agarwal, A., Kakade, S. M., Lee, J. D., and Mahajan, G. Optimality and approximation with policy gradient methods in Markov Decision Processes. *arXiv:1908.00261v2*, August 2019. [2](#), [15](#), [16](#), [17](#), [18](#), [19](#), [20](#), [25](#), [26](#), [27](#)
- Antos, A., Szepesvári, Cs., and Munos, R. Learning near-optimal policies with Bellman-residual minimization based fitted policy iteration and a single sample path. *Machine Learning*, 71:89–129, 2008. [4](#)
- Asadi, K., Cater, E., Misra, D., and Littman, M. L. Equivalence between wasserstein and value-aware model-based reinforcement learning. In *FAIM Workshop on Prediction and Generative Modeling in Reinforcement Learning*, 2018. [31](#)
- Bagnell, J. A., Kakade, S., Ng, A. Y., and Schneider, J. Policy search by dynamic programming. In Thrun, S., Saul, L., and Schölkopf, B. (eds.), *Advances in Neural Information Processing Systems (NIPS - 16)*. MIT Press, Cambridge, MA, 2004. [18](#)
- Baxter, J. and Bartlett, P. L. Infinite-horizon policy-gradient estimation. *Journal of Artificial Intelligence Research (JAIR)*, 15:319–350, 2001. [4](#)
- Beck, A. *First-Order Methods in Optimization*. Society for Industrial and Applied Mathematics, 2017. [16](#), [19](#)
- Bertsekas, D. P. Approximate policy iteration: A survey and some new methods. *Journal of Control Theory and Applications*, 9(3):310–335, 2011. [4](#)
- Bhandari, J. and Russo, D. Global optimality guarantees for policy gradient methods. *CoRR*, abs/1906.01786, 2019. [15](#)
- Bhatnagar, S., Sutton, R. S., Ghavamzadeh, M., and Lee, M. Natural actor-critic algorithms. *Automatica*, 45(11):2471–2482, 2009. [4](#)
- Brockman, G., Cheung, V., Pettersson, L., Schneider, J., Schulman, J., Tang, J., and Zaremba, W. OpenAI Gym, 2016. [22](#)
- Cao, X.-R. A basic formula for online policy gradient algorithms. *Automatic Control, IEEE Transactions on*, 50(5):696–699, 2005. [4](#)
- Chen, J. and Jiang, N. Information-theoretic considerations in batch reinforcement learning. In *Proceedings of the 36th International Conference on Machine Learning (ICML)*, 2019. [4](#)
- Chua, K., Calandra, R., McAllister, R., and Levine, S. Deep reinforcement learning in a handful of trials using probabilistic dynamics models. In *Advances in Neural Information Processing Systems*, pp. 4754–4765, 2018. [24](#)
- Deisenroth, M. P., Neumann, G., and Peters, J. A survey on policy search for robotics. *Foundations and Trends in Robotics*, 2(1-2):1–142, 2013. [4](#)
- Deisenroth, M. P., Fox, D., and Rasmussen, C. E. Gaussian processes for data-efficient learning in robotics and control. *IEEE Transactions on Pattern Analysis and Machine Intelligence*, 37(2): 408–423, 2015. [1](#)

- D’Oro, P., Metelli, A. M., Tirinzoni, A., Papini, M., and Restelli, M. Gradient-aware model-based policy search. *arXiv preprint arXiv:1909.04115*, September 2019. 2, 7
- Ernst, D., Geurts, P., and Wehenkel, L. Tree-based batch mode reinforcement learning. *Journal of Machine Learning Research (JMLR)*, 6:503–556, 2005. 4
- Farahmand, A.-m. Iterative value-aware model learning. In *Advances in Neural Information Processing Systems (NeurIPS - 31)*, pp. 9072–9083, 2018. 2, 4, 30, 31
- Farahmand, A.-m. and Precup, D. Value pursuit iteration. In Pereira, F., Burges, C., Bottou, L., and Weinberger, K. (eds.), *Advances in Neural Information Processing Systems (NIPS - 25)*, pp. 1349–1357. Curran Associates, Inc., 2012. 4
- Farahmand, A.-m., Ghavamzadeh, M., Szepesvári, Cs., and Mannor, S. Regularized fitted Q-iteration for planning in continuous-space Markovian Decision Problems. In *Proceedings of American Control Conference (ACC)*, pp. 725–730, June 2009. 4
- Farahmand, A.-m., Precup, D., Ghavamzadeh, M., and Barreto, A. M. Classification-based approximate policy iteration. *IEEE Transactions on Automatic Control*, 60(11):2989–2993, November 2015. 18
- Farahmand, A.-m., Barreto, A. M., and Nikovski, D. N. Value-aware loss function for model learning in reinforcement learning. In *13th European Workshop on Reinforcement Learning (EWRL)*, December 2016a. 4, 30
- Farahmand, A.-m., Ghavamzadeh, M., Szepesvári, Cs., and Mannor, S. Regularized policy iteration with nonparametric function spaces. *Journal of Machine Learning Research (JMLR)*, 17(139): 1–66, 2016b. 4
- Farahmand, A.-m., Barreto, A. M., and Nikovski, D. N. Value-aware loss function for model-based reinforcement learning. In *Proceedings of the 20th International Conference on Artificial Intelligence and Statistics (AISTATS)*, pp. 1486–1494, April 2017. 2, 4, 30, 31
- Farquhar, G., Rocktaeschel, T., Igl, M., and Whiteson, S. TreeQN and ATreeC: Differentiable tree planning for deep reinforcement learning. In *International Conference on Learning Representations (ICLR)*, 2018. 2
- Ghavamzadeh, M. and Engel, Y. Bayesian policy gradient algorithms. In Schölkopf, B., Platt, J., and Hoffman, T. (eds.), *Advances in Neural Information Processing Systems (NIPS - 19)*, pp. 457–464. MIT Press, Cambridge, MA, 2007. 4
- Gordon, G. Stable function approximation in dynamic programming. In *International Conference on Machine Learning (ICML)*, 1995. 4
- Ha, D. and Schmidhuber, J. Recurrent world models facilitate policy evolution. In *Advances in Neural Information Processing Systems (NeurIPS - 31)*, pp. 2455–2467, 2018. 1
- Huang, D.-A., Farahmand, A.-m., Kitani, K. M., and Bagnell, J. A. Approximate MaxEnt inverse optimal control and its application for mental simulation of human interactions. In *AAAI Conference on Artificial Intelligence*, January 2015. 27

- Joseph, J., Geramifard, A., Roberts, J. W., How, J. P., and Roy, N. Reinforcement learning with misspecified model classes. In *Proceedings of IEEE International Conference on Robotics and Automation (ICRA)*, pp. 939–946. IEEE, 2013. 2
- Kakade, S. A natural policy gradient. In *Advances in Neural Information Processing Systems (NIPS)*, pp. 1531–1538, 2001. 4
- Kakade, S. and Langford, J. Approximately optimal approximate reinforcement learning. In *Proceedings of the Nineteenth International Conference on Machine Learning (ICML)*, pp. 267–274, 2002. 16, 18
- Kingma, D. P. and Ba, J. Adam: A method for stochastic optimization. *arXiv preprint arXiv:1412.6980*, 2014. 33
- Kurutach, T., Clavera, I., Duan, Y., Tamar, A., and Abbeel, P. Model-ensemble trust-region policy optimization. *arXiv preprint arXiv:1802.10592*, 2018. 24
- Lagoudakis, M. G. and Parr, R. Least-squares policy iteration. *Journal of Machine Learning Research (JMLR)*, 4:1107–1149, 2003a. 4
- Lagoudakis, M. G. and Parr, R. Reinforcement learning as classification: Leveraging modern classifiers. In *Proceedings of the 20th International Conference on Machine Learning (ICML)*, pp. 424–431, 2003b. 18
- Lazaric, A., Ghavamzadeh, M., and Munos, R. Analysis of a classification-based policy iteration algorithm. In *Proceedings of the 27th International Conference on Machine Learning (ICML)*, pp. 607–614. Omnipress, 2010. 18
- Lazaric, A., Ghavamzadeh, M., and Munos, R. Finite-sample analysis of least-squares policy iteration. *Journal of Machine Learning Research (JMLR)*, 13:3041–3074, October 2012. 4
- Lazaric, A., Ghavamzadeh, M., and Munos, R. Analysis of classification-based policy iteration algorithms. *Journal of Machine Learning Research (JMLR)*, 17(19), 2016. 18
- Lillicrap, T. P., Hunt, J. J., Pritzel, A., Heess, N., Erez, T., Tassa, Y., Silver, D., and Wierstra, D. Continuous control with deep reinforcement learning. *arXiv preprint arXiv:1509.02971*, 2015. 7, 21, 23, 24, 33
- Liu, B., Cai, Q., Yang, Z., and Wang, Z. Neural proximal/trust region policy optimization attains globally optimal policy. In *Advances in Neural Information Processing Systems (NeurIPS - 32)*, pp. 10564–10575. 2019. 15
- Luo, Y., Xu, H., Li, Y., Tian, Y., Darrell, T., and Ma, T. Algorithmic framework for model-based deep reinforcement learning with theoretical guarantees. *arXiv preprint arXiv:1807.03858*, 2018. 2
- Marbach, P. and Tsitsiklis, J. N. Simulation-based optimization of Markov reward processes. *Automatic Control, IEEE Transactions on*, 46(2):191–209, February 2001. 4

- Mnih, V., Kavukcuoglu, K., Silver, D., Rusu, A. A., Veness, J., Bellemare, M. G., Graves, A., Riedmiller, M., Fidjeland, A. K., Ostrovski, G., Petersen, S., Beattie, C., Sadik, A., Antonoglou, I., King, H., Kumaran, D., Wierstra, D., Legg, S., and Hassabis, D. Human-level control through deep reinforcement learning. *Nature*, 518(7540):529–533, February 2015. 4
- Müller, A. Integral probability metrics and their generating classes of functions. *Advances in Applied Probability*, 29(2):429–443, 1997. 31
- Munos, R. and Szepesvári, Cs. Finite-time bounds for fitted value iteration. *Journal of Machine Learning Research (JMLR)*, 9:815–857, 2008. 4
- Nagabandi, A., Kahn, G., Fearing, R. S., and Levine, S. Neural network dynamics for model-based deep reinforcement learning with model-free fine-tuning. In *2018 IEEE International Conference on Robotics and Automation (ICRA)*, pp. 7559–7566. IEEE, 2018. 24
- Oh, J., Singh, S., and Lee, H. Value prediction network. In *Advances in Neural Information Processing Systems (NIPS - 30)*, pp. 6118–6128. Curran Associates, Inc., 2017. 2
- Peng, J. and Williams, R. J. Efficient learning and planning within the Dyna framework. *Adaptive Behavior*, 1(4):437–454, 1993. 1
- Peters, J. and Schaal, S. Natural actor-critic. *Neurocomputing*, 71(7):1180–1190, 2008. 4
- Peters, J., Sethu, V., and Schaal, S. Reinforcement learning for humanoid robotics. In *Humanoids2003, Third IEEE-RAS International Conference on Humanoid Robots*, 2003. 4
- Scherrer, B., Ghavamzadeh, M., Gabillon, V., and Geist, M. Approximate modified policy iteration. In *Proceedings of the 29th International Conference on Machine Learning (ICML)*, 2012. 4
- Schulman, J., Levine, S., Abbeel, P., Jordan, M., and Moritz, P. Trust region policy optimization. In *International Conference on Machine Learning (ICML)*, 2015. 4, 7
- Shani, L., Efroni, Y., and Mannor, S. Adaptive trust region policy optimization: Global convergence and faster rates for regularized MDPs. *arXiv preprint arXiv:1909.02769*, September 2019. 15
- Silver, D., Lever, G., Heess, N., Degris, T., Wierstra, D., and Riedmiller, M. Deterministic policy gradient algorithms. In *International Conference on Machine Learning (ICML)*, 2014. 7
- Silver, D., Schrittwieser, J., Simonyan, K., Antonoglou, I., Huang, A., Guez, A., Hubert, T., Baker, L., Lai, M., Bolton, A., Chen, Y., Lillicrap, T., Hui, F., Sifre, L., Driessche, G. v. d., Graepel, T., and Hassabis, D. Mastering the game of go without human knowledge. *Nature*, 550(7676):354–359, 10 2017a. 18
- Silver, D., van Hasselt, H., Hessel, M., Schaul, T., Guez, A., Harley, T., Dulac-Arnold, G., Reichert, D., Rabinowitz, N., Barreto, A. M., and Degris, T. The predictron: End-to-end learning and planning. In *Proceedings of the 34th International Conference on Machine Learning (ICML)*, pp. 3191–3199, 2017b. 2
- Sutton, R. S. Integrated architectures for learning, planning, and reacting based on approximating dynamic programming. In *Proceedings of the 7th International Conference on Machine Learning (ICML)*, 1990. 1, 3

- Sutton, R. S., McAllester, D., Singh, S., and Mansour, Y. Policy gradient methods for reinforcement learning with function approximation. In *Advances in Neural Information Processing Systems (NIPS - 12)*, 2000. [4](#), [5](#)
- Sutton, R. S., Szepesvári, Cs., Geramifard, A., and Bowling, M. Dyna-style planning with linear function approximation and prioritized sweeping. In *Proceedings of the 24th Conference on Uncertainty in Artificial Intelligence (UAI)*, 2008. [1](#)
- Szepesvári, Cs. *Algorithms for Reinforcement Learning*. Morgan Claypool Publishers, 2010. [3](#)
- Szepesvári, Cs. and Smart, W. D. Interpolation-based Q-learning. In *Proceedings of the twenty-first International Conference on Machine Learning (ICML)*, 2004. [4](#)
- Talvitie, E. Self-correcting models for model-based reinforcement learning. In *Proceedings of the Thirty-First AAAI Conference on Artificial Intelligence*, pp. 2597–2603, 2017. [1](#)
- Tosatto, S., Pirotta, M., D’Eramo, C., and Restelli, M. Boosted fitted Q-iteration. In *Proceedings of the 34th International Conference on Machine Learning (ICML)*, 2017. [4](#)
- Williams, R. J. Simple statistical gradient-following algorithms for connectionist reinforcement learning. *Machine Learning*, 8(3-4):229–256, 1992. [4](#), [7](#), [21](#)